ŁUKASIEWICZ RESEARCH NETWORK
INSTITUTE OF ELECTRONIC MATERIALS TECHNOLOGY

MATERIAŁY ELEKTRONICZNE

ELECTRONIC MATERIALS

QUARTERLY

Vol. 47, No. 1 - 4
2019

WARSAW ŁUKASIEWICZ – ITME 2019

MATERIAŁY ELEKTRONICZNE
ELECTRONIC MATERIALS

Vol. 47 No. 1 - 4 2019

CONTENTS

Maintaining the English language version of the journal „Electronic Materials" and introducing the identification to the journal „Electronic Materials" through the Digital Object Identifier are tasks financed in accordance with the 686/P-DUN/2019 agreement from the funds of the Ministry of Science and Higher Education intendend for the science dissemination.

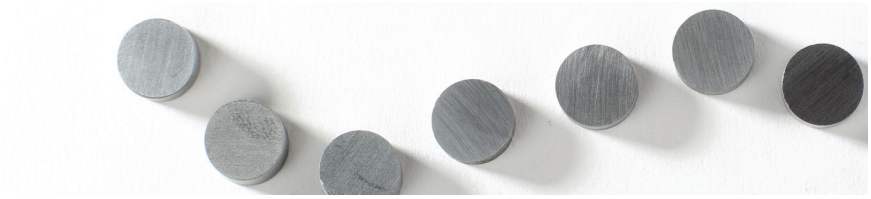

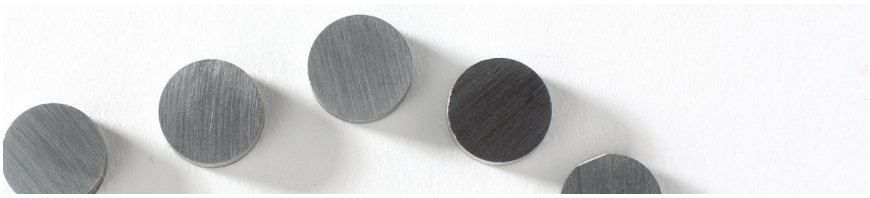

On the cover:
Ag-C composites developed as a part of the GRAMCOM project.

EDITORIAL OFFICE ADDRESS

Łukasiewicz Research Network - Institute of Electronic Materials Technology
Wólczyńska Str. 133, 01-919 Warsaw
e-mail: ointe@itme.edu.pl
www: matelektron.itme.edu.pl

PL ISSN 0209 - 0058

CONTACT

Editor in Chief phone: (22) 639 58 85
Editorial Assistant phone: (22) 639 55 29

A quarterly quoted on the list of scientific journals of the Ministry of Science and Higher Education
7 points - according to the statement of the Ministry of Science and Higher Education.

Published articles are indexed in databases:
BazTech, CAS - Chemical Abstracts

Published articles of a scientific nature are reviewed by independent researchers.

The paper version is the primary version.

The quarterly is published in open access.

Circulation: 200 copies

Thermal analysis (TG, DSC) and specific heat (Cp) measurements

The Department of Composites and Ceramic Materials

STA 449 F5 Jupiter TG-DTA/DSC Thermal Analyzer

Facilities:

Differential Scanning Calorimetry (DSC) is conducted. True TGA and DSC measurements can be performed at sample temperatures from ambient to 1600°C. TGA measurements are also possible, even on large or heavy samples.

Parameters:

- Temperature range: RT - 1600°C
- Temperature resolution: 0.001 K
- Heating rate: 0.001 to 50 K/min
- Atmospheres: inert, oxidizing, static, dynamic, vacuum

Sample size:

- Maximum sample load: 35 g (incl. crucible)
- Sample volume: up to 5 cm^3

RESEARCH NETWORK ŁUKASIEWICZ

Insitute of Electronic Materials Technology

Wólczyńska 133,
01-919 Warszawa

+48 22 835 30 41
+48 22 639 58 05

itme@itme.edu.pl
komercjalizacja@itme.edu.pl

Influence of the rigid alumina particles added to ZrO_2 ceramics stabilized with Y_2O_3 for its mechanical properties

Marek Boniecki[1], Przemysław Gołębiewski[1], Helena Węglarz[1], Anna Piątkowska[1], Magdalena Romaniec[1], Konrad Krzyżak[1]

The effect of the phase added to ZrO_2 ceramics on its mechanical properties, and in partcular on the fracture toughness, was examined using the example of Al_2O_3 - ZrO_2 composite where ZrO_2 was stabilized with 3 mol% of Y_2O_3. Composites of 20% wt. Al_2O_3 - 80 wt.% ZrO_2 with different size of corundum grain were made. Vickers indenter crack resistance tests showed an increase of 21% in the value of this parameter for the samples with Al_2O_3 grains of approx. 6.5 μm in comparison with pure ZrO_2 ceramics. On the basis of literature data and microscopic observations, authors present a thesis that this increase is caused by two factors, i.e. the increase of the phase transition range (from tetragonal to monoclinic phase) accompanying crack propagation and the effect of large Al_2O_3 grains as bridges fastening the fracture surfaces.

Key words: ZrO_2 ceramics stab. 3 mol. %Y_2O_3, ceramic additives with a large Young's modulus, Al_2O_3 grain sizes, fracture toughness, bending strength

Wpływ sztywnych korundowych cząstek dodawanych do ceramiki ZrO_2 stabilizowanej Y_2O_3 na jej właściwości mechaniczne

Wpływ fazy dodawanej do ceramiki ZrO_2 na jej właściwości mechaniczne w tym głównie na jej odporność na pękanie zbadano na przykładzie kompozytu Al_2O_3 – ZrO_2 gdzie ZrO_2 było stabilizowane 3% mol Y_2O_3. Wykonano kompozyty 20% wag. Al_2O_3 – 80% wag. ZrO_2 różniące się wielkością ziarna korundowego. Badania odporności na pękanie prowadzone metodą wgłębnika Vickersa wykazały wzrost wielkości tego parametru o 21% dla próbek z ziarnami Al_2O_3 o wielkości ok. 6,5 μm w porównaniu z czystą ceramiką ZrO_2. Na podstawie danych literaturowych oraz własnych obserwacji mikroskopowych postawiono tezę, że wzrost ten spowodowany jest przez dwa czynniki tj. zwiększenie się zakresu przemiany fazowej (z fazy tetragonalnej do jednoskośnej) towarzyszącej propagacji pęknięcia oraz działaniem dużych ziaren Al_2O_3 jako mostków spinających powstające powierzchnie przełamu.

Słowa kluczowe: ceramika ZrO_2 stab. 3% mol. Y_2O_3, dodatki ceramiczne o dużym module Younga, wielkość ziaren Al_2O_3, odporność na pękanie, wytrzymałość na zginanie

DOI: https://doi.org/10.34769/g9x6-7e09

1. Introduction

In comparison with the most structural material such as steel, ceramic are characterised by lower density, significantly higher resistance to various corrosive factors, such as high temperature and abrasion. Ceramic elements can be used as cutting tools, crucibles for melting metals and glass, as tools for semiconductor production, catalyst carriers for removing pollutants from car exhausts, as parts for car engines, turbochargers, brake discs, etc. [1-2]. Ceramics are also used for biomedical purposes (prostheses) [3] as well as transparent ceramics for making laser bars, windows or lenses [4].

The main obstacle to the wide use of ceramics as a structural material is primarily its brittle fracture, which can cause unexpected destruction of the element made of the material resulting from the development of subcritical cracks caused by applied stress [5]. In order to increase the resistance to cracking, we can use additives e.g. in the form of metal particles [6], fibers [7], carbon nanotubes [8], graphene flakes [9-12] or ceramic particles with higher stiffness (larger Young's modulus) than the matrix [13-25].

The aim of the work was to obtain ZrO_2 based composites with a high fracture toughness resulting from the introduction of the rigid ceramic particles (particles with high Young's modulus) to the zirconia matrix (stabilized with 3 mol% Y_2O_3). To prezent the example of such particles, Al_2O_3 grains were selected and then added to the ZrO_2 matrix (20% by weight which corresponds to a volume content of 28%).

2. Work hypotheses and literature review

The following hypotheses will be proved in this work: The overall fracture toughness K_{Ic} of zirconia based

[1] *Łukasiewicz Research Network - Institute of Electronic Materials Technology*, 133 Wólczyńska Str., 01-919 Warsaw, Poland e-mail: marek.boniecki@itme.edu.pl

Tab. 1. K_{Ic} for 3Y-TZP from literature.
Tab. 1. K_{Ic} dla 3Y-TZP na podstawie literatury.

K_{Ic} (MPam$^{1/2}$)	4.4	7.6	2.5	5 ± 0.5 (MED)	5.05 ± 0.03 (MED) 5.97 ± 0.06 (PQ)	5.5 ± 0.2 (MED)
Ref.	[11]	[14]	[16]	[20]	[23]	[31]
Formula for calculation	Anstis [29]	Anstis [29]	Anstis [29]	Niihara [30]	Niihara [30]	Niihara [30]

Tab. 2. Some properties of ceramics added to 3Y-TZP. The properties of 3Y-TZP are presented for comparison. Data sources are given in square brackets.
Tab. 2. Niektóre właściwości faz ceramicznych dodawanych do 3Y-TZP. Dla porównania pokazano właściwości ceramiki 3Y-TZP. W nawiasach kwadratowych podane są źródła danych.

Material → **Properties ↓**	**ZrO_2 matrix**	**Al_2O_3**	**SiC [34]**	**TiC [35]**	**WC**	**TiB_2**
E (GPa)	205 ± 4 [31]	370 ± 14 [31]	410	450	700 [22]	560 [35]
α (10^{-6}/°C)	10 (300 - 2000 K) [16]	8.6 (300 - 1800 K) [33]	4.0	8.5	5.2 [22]	5 (300 - 800 K) 9 (950 - 2000 K) [16]
ρ (g/cm^3)	6.1 [26]	3.98 [33]	3.1	4.93	15.7 [18]	4.52 [35]
H (GPa)	13.8 [31]	15 [33]	28	28	26 [36]	26 [35]

where : E is a Young's modulus, α is a coefficient of thermal expansion (CTE), ρ is a density and H is a Vickers hardness.

composites with rigid ceramic particles can be expressed as:

$$K_{Ic} = K_0 + \Delta K_{IcT} + \Delta K_{IcD} + \Delta K_{IcB} + \Delta K_{IcO} \quad (1)$$

where K_0 is the inherent matrix toughness, i.e. the zirconia matrix without or with negligible transformation toughening, ΔK_{IcT} is the transformation toughening contribution, ΔK_{IcD} is the toughening due to crack deflection caused mainly by the rigid ceramic particles, ΔK_{IcB} is the toughening due to crack bridging and ΔK_{IcO} is the toughening due to other mechanisms for example crack branching.

ZrO_2 can be found in three polymorphic forms [26]. The stable polymorph at low temperatures has monoclinic structure. In the medium temperature range the tetragonal phase occurs. In the area of maximum to melting temperatures (2983 K), a stable phase of regular fluorite structur can be observed. The transformation of the tetragonal phase to monoclinic leeds to the appearence of cracks generated by the stress which is associated with volume expansion of 3 - 5%. It was found that annealing at high temperatures (1273-1773 K) in the presence of some oxides to stabilize the tetragonal or regular ZrO_2. The examples of the commonly used stabilizing oxides are: CaO, MgO, CeO_2 or Y_2O_3 (the last one is the most often used). These oxides formed with ZrO_2 solid solution, where in place of zirconium ions oxide cations are embedded. The addition of the oxides to ZrO_2 lowers the temperature of polymorphic transformations, reduces the volume changes and blocks the transformation. The metastable phases: regular or tetragonal are obtained. The last one has very good mechanical properties, ie. high bending strength and fracture toughness [27-28] which originate from the stress-induced transformation of the tetragonal phase to monoclinic in the stress field of propagating cracks, a phenomenon known as transformation toughening (ΔK_{IcT} in (1)).

In this work 3 mol% Y_2O_3 stabilized tetragonal ZrO_2 (3Y-TZP) is proposed to be the ceramic matrix. In Tab. 1 there are some values of fracture toughness K_{Ic} for 3Y-TZP found in literature. In this case $K_{Ic} = K_0 + \Delta K_{IcT0}$ (where ΔK_{IcT0} means ΔK_{IcT} in (1) for ZrO_2 matrix).

K_{Ic} was determined using surface cracks made by Vickers indentation. The values were obtained using different formulas. Value 2.5 MPam$^{1/2}$ in [16] can be accepted as K_0 because only very small amount of monoclinic ZrO_2 was revealed on the fracture surfaces (hence $\Delta K_{IcT0} \approx 0$). K_{Ic} in [20, 23, 31] was calculated by Niihara median (MED) and Palmqvist (PQ) equation.

The values of K_{Ic} in Tab.1 in comparison with the value for steel, which is a very popular structural material ($K_{Ic} \approx$ 40 MPam$^{1/2}$ [32]), are several times smaller. In order to increase K_{Ic} of 3Y-TZP it is suggested to introduce rigid ceramic particles. It should induce several toughening mechanisms such as: crack deflection, branching or bridging of crack surfaces and it can also increase the ΔK_{IcT} share, which is shown later in the text. As result we can observe a significant increase in the fracture toughness of the composites.

On the basis of literature data [13-25] some ceramic particles used for reinforcement of 3Y-TZP are shown in Tab. 2.

All the ceramics added to 3Y-TZP have bigger E and H but smaller α than ZrO_2. As a consequence the residual thermal stresses are generated in composites during the process of cooling from sintering to room temperature [16, 21-25]. There are tensile in 3Y-TZP and compressive stresses in the added particles. For example, for the 30 vol.% TiB_2 - 70 vol.% ZrO_2 composite [16], the tensile stress in the matrix was estimated to be 0.26 GPa. On the other hand, for composites 10 vol.% Al_2O_3 - 90 vol.% ZrO_2 and 10 vol.% WC - 90 vol.% ZrO_2 [21] the maximum tensile stress in the matrix was 1.02 and 1.56 GPa respectively, and compressive stress in Al_2O_3 and WC respectively 0.66 and 1.35 GPa. The calculations of residual tensile stress in the ZrO_2 matrix (using the expression from [37]) gave the value of 0.44 GPa. In these calculations data for ZrO_2 and Al_2O_3 from Tab. 2 but Poisson's ratio equals 0.3 and 0.22 respectively. The residual tensile stresses in 3Y-TZP enhance its transformability and therefore the transformation toughening (ΔK_{IcT} in Eq.(1)). The influence of the residual stresses on transformation toughness could be explained in the following way:

Tab. 3. Relative improvement of fracture toughness ΔK_{Ic} of 3Y-TZP as a result of the introduction of the rigid particles (based on literature).

Tab. 3. Wzrost odporności na pękanie ΔK_{Ic} ceramiki 3Y-TZP wskutek wprowadzania do niej cząstek metalicznych (na podstawie literatury).

Particle material	Content (vol.%)	Grain size of additives (μm)	ΔK_{Ic} (%)	remarks	Ref.
Al_2O_3	30	6.5	30		[13]
Al_2O_3	20	3.0	64		[14]
Al_2O_3	10	-	20		[21]
SiC	5	0.15	11		[24]
TiC	20	1.84	17		[25]
WC	30	0.13 ± 0.05	46	*	[17]
WC	20	2.0	26	*	[18]
WC	20	1.6 ± 0.6	104	*	[19]
WC	10	0.13 ± 0.6	111	*	[19]
WC	10	1.82	30		[20]
WC	10	0.12	70		[20]
WC	10	-	60		[21]
WC	32	1.49	43		[23]
TiB_2	20	1.5 – 2.0	23		[15]
TiB_2	30	1.5 – 2.0	76		[16]

Where: ΔK_{Ic} (%) = $\Delta K_{Ic}/(\Delta K_{IcT0})$, * - ZrO_2 in these articles was stabilized by 2.8% Y_2O_3.

In the presence of tensile residual stress σ_r, the critical stress σ_{cT} required to initiate the stress-induced transformation in the crack tip would be reduced to σ_{cT}^m:

$$\sigma_{cT}^m = \sigma_{cT} - \sigma_r \,. \tag{2}$$

The reduction in critical stress would actually contribute to the development of a larger transformation zone h according to the formula proposed in [38]:

$$h \sim (\sigma_{cT}^m)^{-2} \,. \tag{3}$$

The increased transformation zone size enhances the transformation toughening contribution [39]:

$$\Delta K_{IcT} \sim h^{1/2} \sim (\sigma_{cT}^m)^{-1}. \tag{4}$$

Hence ΔK_{IcT} is usually bigger than ΔK_{IcT0} for zirconia matrix.

The presence of secondary rigid particles in zirconia based composites causes crack deflection toughening mechanism which, for example, for 30 vol.% TiB_2 content in [16] increase the fracture toughness of about 15%. It could also cause crack bridging toughening because the grains of the additives (Tab. 3) are usually larger than the 3Y-TZP grains (0.3 - 0.5 μm [16]) and they are under the compressive strength in matrix. In this situation they could play a role of the bridges connecting the surfaces of the crack behind the head of the propagating crack. Tab. 3 presents the literature data of improvement of fracture toughness for 3Y-TZP reinforced by introducing rigid particles of various ceramics.

In the case of the addition of Al_2O_3 [13-14], an increase of fracture toughness was a function of the grain size. The data in Tab. 3 refer to the largest grain sizes used in [13-14]. Bending strength of the composites is usually not worse than for matrix ceramics. It is above 1 GPa [16, 20-21, 23-25].

3. Experimental part

3.1. Preparation of samples

The starting materials in our experiments were: commercial powder ZrO_2 stab. 3 mol.% Y_2O_3 delivered by Tosoh labelled as TZ-3Y-E with a purity of about 99.9% and crystal sizes 40 nm and Sumitomo Al_2O_3 powders with a purity of 99.99% designated as AA-04 and AA-18 with different grain sizes was used as starting materials. A mixture of powders in a proportion of 20 wt.% Al_2O_3 and 80 wt.% ZrO_2 as well as pure ZrO_2 powder (for making the matrix) were placed in a planetary mill in a container of stabilized ZrO_2 with balls with a diameter of 5 mm made from above material. The deionized water together with the plasticizer (Dolapix CE64) was added to the powder in an amount allowing to obtain a slurry with a content of 75% by weight of dry matter, and then stirred for

one hour at a speed of 150 rpm. After adding the binder (Duramax B1000) the suspension was stirred for 30 min at 100 rpm. The granules prepared in this way were made using cryogenic granulation method. 65 × 40 × 8 mm shaped moldings were pressed from the granulates, which were densified with isostatic pressure of 120 MPa. The moldings were sintered in two stages: initially at 800ºC, then at 1480ºC for 2 h (in air). The sintered bodies were cut and ground into beams for measuring mechanical properties. Part of the beams was polished unilaterally.

3.2. Tests of mechanical properties

The aim of our work was to measure fracture toughness K_{Ic}, bending strength σ_c, Young's modulus E and Vickers hardness H were measured. K_{Ic} measurements were carried out using three methods:

(a) By three-point bending of notched beams:

The measurements were carried out on 2.5 mm × 4 mm × 30 mm beams. The beams were cut in the middle (along the side of a length of 4 mm) to a depth of 0.9 mm using a circular saw with a thickness of 0.2 mm, and then to a depth of 0.2 mm with a disk thickness of 0.025 mm. The distance of the L supports was 20 mm. The samples were loaded with a crosshead displacement speed of 1 mm/min. The K_{Ic} value was calculated from the formula:

$$K_{Ic} = Y \frac{1.5 P_c L}{b w^2} \; c_k^{0.5}, \tag{5}$$

where: Y - geometrical constant calculated according to [40], P_c - breaking load, b = 2.5 mm - beam width, w = 4 mm - beam height, c_k - notch length (about 1.1 mm)

(b) By measuring the bending strength of the sample with the previously introduced Vickers fracture.

The measurements were carried out on samples with the dimensions described in paragraph (a) with a polished surface of 4 mm × 30 mm. In the centre of the polished surface of the sample, a Vickers indent was made under the load of P = 98.1 N, so that one pair of cracks running from the corners was perpendicular to the edge of the sample. Four-point bending strength test was then performed with a crosshead displacement speed of 1 mm/min, placing the sample in such a way that the introduced crack was on the extended beam surface between the upper pressure rollers. The value of K_{Ic} was calculated from the following formula from [41]:

$$K_{Ic} = 0.59(E/H)^{1/8} (\sigma_c P^{1/3})^{3/4}, \tag{6}$$

where: E - Young's modulus, H - Vickers hardness, P = 98.1 N - Vickers indenter load and σ_c - four-point bending strength calculated from formula (7):

$$\sigma_c = \frac{1.5 P_c (L - l)}{b w^2}, \tag{7}$$

where: P_c - breaking load, L = 20 mm - distance of lower supports, l = 10 mm - distance of upper pressure rollers, b = 4 mm - width, w = 2.5 mm - beam height.

c) K_{Ic} determined on the basis of measuring the length of cracks running from the corners of the Vickers impression.

The value of c, averaged from the measurements of the length of four cracks running from the tops of he indent, is introduced into the appropriate formula given in the literature. The most popular are the formulas given in [29-30]. According to [29]:

$$K_{Ic} = 0.016 \; (E/H)^{0.5} \; P/c^{1.5} \tag{8}$$

where: c - average length of Vickers cracks, the other parameters were defined earlier.

According to [30]:

$$K_{Ic} = \frac{0.129 \mathrm{H} \sqrt{\alpha}}{\varphi} \left(\frac{E\varphi}{H}\right)^{0.4} \left(\frac{c}{\alpha}\right)^{-1.5} \tag{9}$$

where: a - half of the diagonal of a Vickers indent, φ = 3 [30]

K_{Ic} was determined by methods (a) and (b) as the average for 10 beams, In turn for method (c) of 10 Vickers indents measured on beams used subsequently in method (b).

Four-point bending strength σ_c was determined according to [42] with a crosshead displacement speed of 1 mm/min on samples with dimensions of 2 mm × 2.5 mm × 30 mm in the conditions described in point (b). The stretched surface (2.5 mm × 30 mm) was polished. Strength values were calculated from the formula (7) where b = 2.5 mm and w = 2 mm. The test was performed on 30 samples.

Young's E modulus was determined according to [43] by bending three-point beams with dimensions: 1 mm × 4 mm × 50 mm with the support distance L = 40 mm by registering the deflection value of the sample as a function of the applied stress P. The deflection values were recorded using an inductive sensor placed in the deflection arrow of the beam. The load was applied at a constant speed of 1 mm/min to $P_k < P_c$. The test was carried out on 10 samples. The value of E was determined from the formula:

$$E = \frac{L^3}{4 b w^3 C} \tag{10}$$

where: b = 4 mm, w = 1 mm, $C = \Delta y/\Delta P$ (the ratio of the increase in the deflection to the load increase)

All the measurements were made on the modernized Zwick 1446 machine supported by the testXpert III program.

Vickers indents were made on polished surfaces of the samples using a hardness tester equipped with a Vickers indenter. H values were calculated from the formula:

$$H = 1{,}8544 \; P/(2a)^2 \tag{11}$$

where: a – a half of the diagonal of Vickers' indent

3.3. Microscopic assessment of materials microstructure, fractures and cracks from Vickers indents

The microstructure of the samples was analysed on polished and etched sample surfaces. The samples were thermally etched at 1350°C in air for 0.5 h. Photographs of microstructures, notched bar cuts after K_{Ic} test (area close to the cutting face) and Vickers cracking were taken using the AURIGA CrossBeam Workstation scanning electron microscope (Carl Zeiss). The grain sizes were estimated using Feret's diameters by the Clemex Techn. Inc. image analysis program. The results were presented as mean and standard deviation, assuming that the grain sizes are normally distributed.

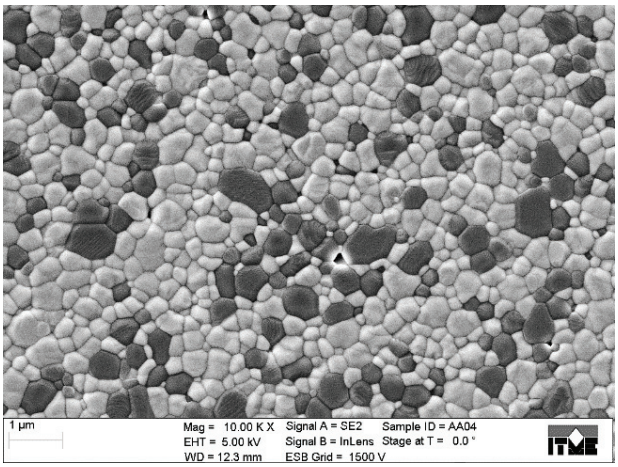

ZrO_2+AA-04

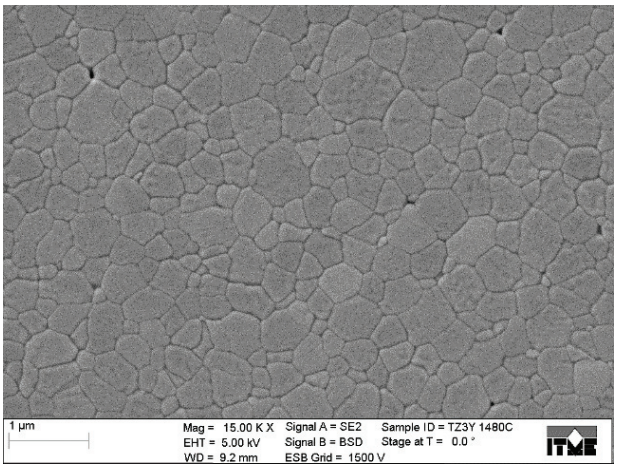

ZrO_2

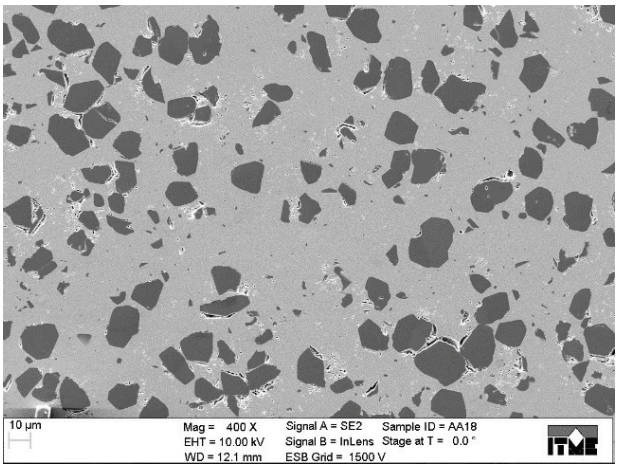

ZrO_2+AA-18

Fig. 1. Microstructure of ZrO_2 samples and composites of 20% wt. Al_2O_3 - 80 wt.% ZrO_2. AA-04 and AA-18 indicated the Al_2O_3 powder types added to the ZrO_2 matrix. The bright grains are ZrO_2 and the dark ones are Al_2O_3.
Rys. 1. Mikrostruktura próbek tworzywa ZrO_2 oraz kompozytów 20% wag. Al_2O_3 – 80% wag. ZrO_2. AA-04 i AA-18 oznaczają rodzaje proszków Al_2O_3 dodane do matrycy ZrO_2. Jasne pola oznaczają ZrO_2, a ciemne Al_2O_3.

Table 4 presents the data characterizing the received materials.

Tab. 4. The size of grains *D* and relative density *d* of the obtained ceramic materials.
Tab. 4. Wielkości ziaren *D* oraz gęstości względne *d* otrzymanych tworzyw ceramicznych.

Material	$D_{Al_2O_3}$ (µm)	D_{ZrO_2} (µm)	*d* (%)
ZrO_2	-	0.41 ± 23	99.7
ZrO_2 + AA-04	0.31 ± 0.18	0.32 ± 0.18	99.8
ZrO_2 + AA-18	6.6 ± 4.1	0.21 ± 0.21	96.5
ZrO_2 + AA-18 1600	6.4 ± 3.2	0.55 ± 0.42	98.0

4. Results and discussion

Pictures of selected microstructures are shown in Fig.1.

Due to the relatively low density of ZrO_2 + AA-18, the additive samples were made from this composition, which were sintered at 1600°C for 2 hours.

In Table 5 the measured mechanical properties of the materials listed in Table 4 were collected, supplemented with ZrO_2 + AA-18 sintered at 1600ºC and 2 composites of 20% wt.%. Al_2O_3 - 80 wt.% ZrO_2 studied in other works.

Numbers in parentheses indicate the formulas from which K_{Ic} was calculated,

* Due to the lack of samples, this K_{Ic} composite was not determined by bending the notched or cracked beams introduced by the Vickers indenter nor as the bending strength or Young's modulus. The *E* value necessary to calculate K_{Ic} using formulas (8,9) was taken in the same way as for ZrO_2 + AA-18.

Material	K_{Ic} (MPam$^{1/2}$)				σ_c	E	H
	(5)	(6)	(8)	(9)	(MPa)	(GPa)	(GPa)
ZrO_2	5.45 ± 0.26	5.07 ± 0.08	3.73 ± 0.10	5.75 ± 0.16	888 ± 83	205 ± 4	13.8
ZrO_2 + AA-04	5.22 ± 0.37	4.73 ± 0.03	3.72 ± 0.20	5.44 ± 0.29	801 ± 203	242 ± 5	15.0
ZrO_2 + AA-18	5.26 ± 0.06	5.40 ± 0.09	4.11 ± 0.35	5.91 ± 0.50	517 ± 49	215 ± 6	11.6
ZrO_2 + AA-18 1600 *	-	-	4.52 ± 0.34	6.51 ± 0.49	-	-	11.6
ZrO_2 + TM-DAR OPUS 11 **	5.17 ± 0.31	4.51 ± 0.07	3.65 ± 0.16	5.33 ± 0.23	-	246 ± 8	15.0
ZrO_2 + Al_2O_3 Tosoh ***	5.46 ± 0.27	-	3.71 ± 0.18	-	1467 ± 262	235 ± 12	15.0

Tab. 5. Mechanical properties of ZrO_2 matrix and composites 20 wt.% Al_2O_3 - 80 wt.% ZrO_2.
Tab. 5. Właściwości mechaniczne matrycy ZrO_2 stabilizowanej 3% mol Y_2O_3 oraz kompozytów 20% wag. Al_2O_3 - 80% wag. ZrO_2.

** The composite was obtained while working on larger research project OPUS 11 No. 2016/21/B/ST8 /01027 implemented on 21/04/2017 in a scientific consortium, of which ITME is a member, and Lublin University of Technology is a leader. The material contains 20 wt.% Taimei corundum ceramics designated as TAIMICRON TM-DAR (the starting powder had a purity of 99.99% and a grain size of about 0.15 μm) and ZrO_2 stab. 3 mol% Y_2O_3 from Tosoh. The grain sizes determined on the polished and etched ceramic surface were 0.25 ± 0.07 and 0.22 ± 0.06 μm for Al_2O_3 and ZrO_2, respectively.

*** Our study concerning the composite was conducted within the framework of ITME statutory theme in 2016. The results were published in [44]. The implementation required a ready-made powder mixture of 20 wt.% Al_2O_3 and 80 wt.% ZrO_2 stab. 3 mol% Y_2O_3 with a purity of 99.9%, a crystallite the size of approx. 29 nm and granules of 60 μm provided by Tosoh. The grain sizes determined on the polished and etched ceramic surface were 0.41 ± 0.23 and 0.27 ± 0.17 μm for Al_2O_3 and ZrO_2, respectively. The high value of σc results from the use of very small test specimens (with a cross-section of 0.95 mm × 1mm × 12 mm at the distance of support of 8 mm).

Due to the low relative density of the ZrO_2 + AA-18 material and thus its relatively high porosity, there was a marked degradation of its mechanical properties (except for K_{Ic}) compared to ZrO_2 + AA-04. Sintering at a higher temperature (1600°C) improved the density and K_{Ic} of the composite with AA-18. The fracture toughness measured with the notched bar method calculated from (5) does not change as a function of the Al_2O_3 grain size, but it gets bigger for samples where the fracture was introduced by the Vickers indenter and when it was measured by the strength method and calculated from (6) and the cracks length was calculated from (8,9). Table 6 summarizes the values of K_{Ic} composites Al_2O_3 - ZrO_2 calculated from formula (8) in the function of the size of introduced Al_2O_3 grains (based on Tab. 4 and 5 and on the description under Tab. 5).

Tab. 6. K_{Ic} calculated according to the formula (8) as a function of Al_2O_3 grain size of the tested materials.
Tab. 6. K_{Ic} obliczane wg wzoru (8) w funkcji wielkości ziarna Al_2O_3 badanych materiałów.

Materiał	$D_{Al_2O_3}$ (μm)	K_{Ic} (MPam$^{1/2}$)
ZrO_2	0	3.73 ± 0.10
ZrO_2 + TM-DAR OPUS 11	0.25 ± 0.07	3.65 ± 0.16
ZrO_2 + AA-04	0.31 ± 0.18	3.72 ± 0.20
ZrO_2 + Al_2O_3 Tosoh	0.41 ± 0.23	3.71 ± 0.18
ZrO_2 + AA-18	6.6 ± 4.1	4.11 ± 0.35
ZrO_2 + AA-18 1600	6.4 ± 3.2	4.52 ± 0.34

The increase in K_{Ic} for ZrO_2 + AA-18 1600 compared to ZrO_2 is around 21%. This result is similar to the one that obtained in [13], where the Al_2O_3 grain size was 6.5 μm and its volume content 30% and the increase in K_{Ic} by 30%. (in our case, the volume content of Al_2O_3 was 28%).

Fig. 2 shows the fracture surfaces of samples formed during the K_{Ic} study on notched beams.

It can be seen that cracks go through the grains of ZrO_2 and Al_2O_3. Photos of the cracks from the Vickers indents in Fig. 3 show that they pass through Al_2O_3 grains confirming fracture observations in Fig. 2.

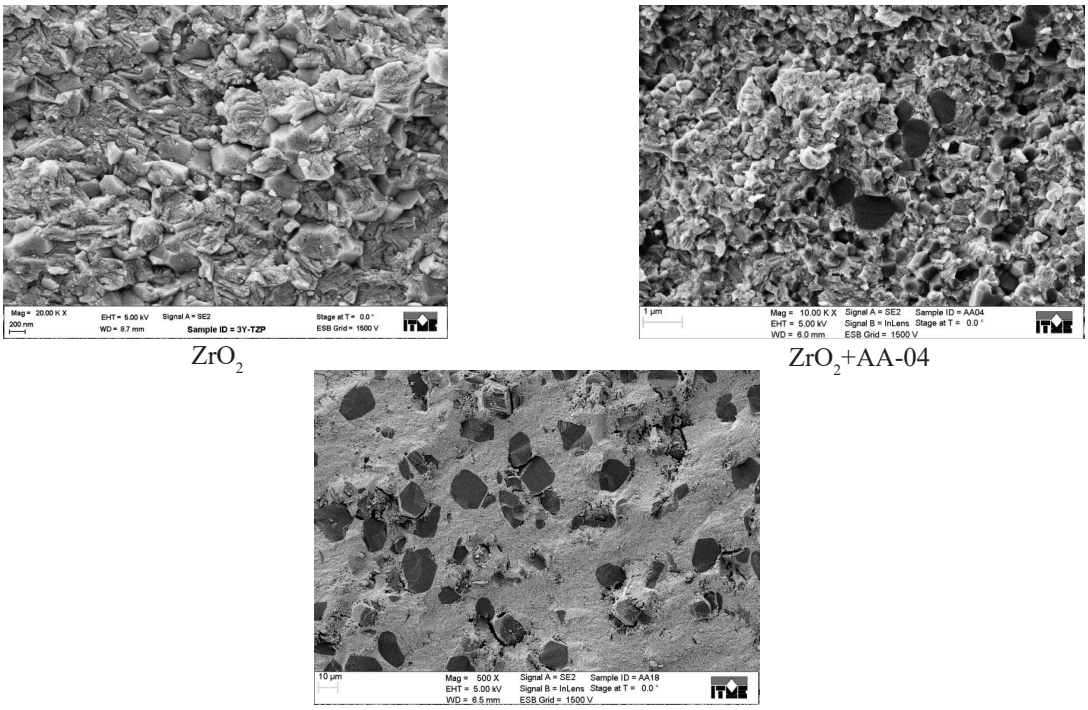

ZrO_2 ZrO_2+AA-04

ZrO_2+AA-18

Fig. 2. Fracture surfaces of samples of ZrO_2 matrix and composites of 20 wt.% Al_2O_3 - 80 wt.% ZrO_2. AA-04 and AA-18 mean the Al_2O_3 powder types added to the ZrO_2 matrix. The bright fields are ZrO_2 and the dark ones are Al_2O_3.
Rys. 2. Przełamy próbek tworzywa ZrO_2 oraz kompozytów 20% wag. Al_2O_3 – 80% wag. ZrO_2. AA-04 i AA-18 oznaczają rodzaje proszków Al_2O_3 dodane do matrycy ZrO_2. Jasne pola oznaczają ZrO_2, a ciemne Al_2O_3.

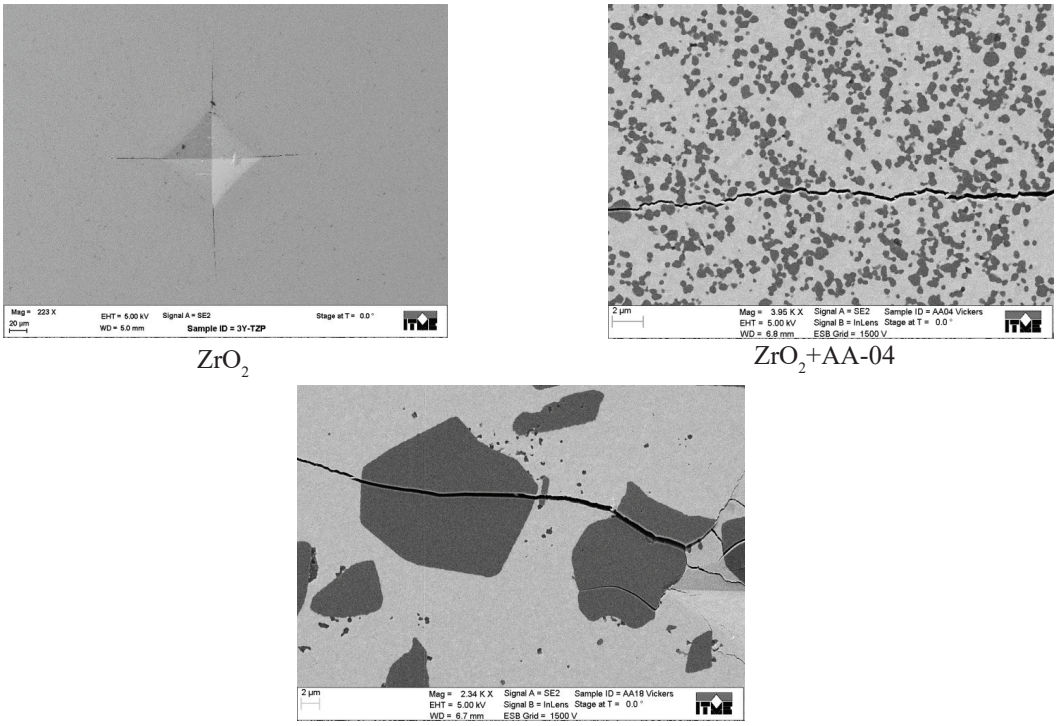

ZrO_2 ZrO_2+AA-04

ZrO2+AA-18

Fig. 3. Cracks from the Vickers indents in samples of ZrO_2 material and composites of 20 wt.% Al_2O_3 - 80 wt.% ZrO_2. The bright fields are ZrO_2 and the dark ones are Al_2O_3.
Rys. 3. Pęknięcia od odcisku Vickersa w próbkach tworzywa ZrO_2 oraz kompozytów 20% wag. Al_2O_3 – 80% wag. ZrO_2. Jasne pola oznaczają ZrO_2, a ciemne Al_2O_3.

The results presented in Tab. 5 and 6 and the microscopic observations in Fig. 2 and 3 are ambiguous. On the one hand, we can see the increase in the number of composites as a function of Al_2O_3 grain size (at least for measurements by the Vickers indenter method), but microscopic observations do not provide clear evidence of deflection of the propagating cracks by Al_2O_3 grains which could be a reason for strenghtening the crack resistance as it was suggested in [13,14]. The fracture toughness K_{Ic} of the composite can be described by Eq. (1).

According to [16] $K_0 = 2.5 \pm 0.1$ MPam$^{1/2}$ (calculated using Eq. (8) from the Vickers indents for $P = 98.1$ N), the basic component of the Eq.(1) is ΔK_{IcT}. Therefore, K_{Ic} should decrease as different materials are added to the matrix. If this is not the case, it means that there is either an increase of ΔK_{IcT} component in the matrix or another toughening mechanism. As indicated in [16,21] material with a coefficient of thermal expansion α smaller than the matrix added to ZrO_2 matrix causes the appearance of local stresses during the cooling of the composite from sintering to room temperature: tensile stress in the matrix and compressive stress in the material being added. For Al_2O_3 α is smaller than for ZrO_2 (Tab.2). In [21] in composite 10 vol.% Al_2O_3 – 90 vol.% ZrO_2 the maximum tensile stress estimated in the matrix was 1.02 GPa, and compressing stress in Al_2O_3 - 0.66 GPa. It was shown in part 2 (Eq. 2 - 4) that the addition of another phase to the matrix with smaller α increases the phase transformation contribution in strengthening the matrix K_{Ic}. There is still no answer to two questions:

1. why do we observe the growth of K_{Ic} (measured by the Vickers method) as a function of the grain size of Al_2O_3?

2. why do not we observe the above increase when using the notched bar method?

Ad. 1. As it can be seen in Fig. 1-3 in the ZrO_2 + AA-18 composite there are large (reaching up to a dozen micrometers) Al_2O_3 grains surrounded by a matrix with submicron grains, which, according to previous considerations, are subjected to compressive stress. These grains can act as bridges connecting the surfaces created in the cracking process. Under the influence of the tensile stress accompanying the propagation of the crack during the pressure of the Vickers indenter, these bridges get broken. The energy needed to destroy the bridges causes an increase in the share of ΔK_{IcB} in the equation (1), and thus the K_{Ic} value for the composite with large Al_2O_3 grains is also increased.

Ad. 2. The measurement procedure, which is the introduction of a precracking by using the sawing method, has a significant influence on the results. The incision at the end has a width of about 25 μm. Propagation of the crack from the face of the incision initiated by the applied external tensile stress begins with a defect resulting from the cutting process. What is important in this process of a crack initiation is the situation in the immediate vicinity of defect. As mentioned earlier it is accompanied by phase transformation. In the case of the composite with AA-04, the fine corundum grains are distributed more densely and then the material near this defect can be considered a composite in which the increase of ΔK_{IcT} (described before) compensates for a 20% weight loss of ZrO_2. On the other hand, in the case of the composite with AA-18, large corundum grains are distributed less often and the material near this defect may be considered as ZrO_2; K_{Ic} values are similar to the values obtained for pure ceramics. Therefore for the three cases considered pure ZrO_2 and ZrO_2 with additions of AA-04 and AA-18, the similar K_{Ic} values are obtained within the error limits (Tab. 5).

5. Summary

This work presents the results of our study on the mechanical properties, and in particular the fracture toughness K_{Ic} of ZrO_2 ceramics stabilized with 3 mol% Y_2O_3 and composites with 20 wt.% Al_2O_3 - 80 wt.% ZrO_2. Two corundum powders of various grain sizes were used. Four materials: pure ZrO_2, composite with Al_2O_3 with grain size of approx. 0.3 μm and 2 composites with Al_2O_3 with a grain size of approx. 6.5 μm sintered at 1480 and 1600°C were obtained. An increase in K_{Ic} by 21% compared to a ZrO_2 matrix was found for a composite with a grain size of approx. 6.5 μm sintered at 1600°C. On the basis of literature data and our own microscopic observations, the thesis was made that this increase is caused by two factors: an increase in the phase transition range (from tetragonal to monoclinic phase) accompanying crack propagation as well as due to the operation of large Al_2O_3 grains asbridges fastening fracture surfaces.

Acknowledgments

This work was financially supported by the research fund of the Institute of Electronic Materials Technology (ITME) in 2018. The authors would like to thank Mr Andrzej Gładki for carrying out calculation of grain size distribution in the studied ceramics.

References

[1] Okada A.: Automotive and industrial applications of structural ceramics in Japan, *J.Eur.Ceram.Soc.*, 2008, 28, 1097-1104.

[2] Okada A.: Ceramic technologies for automotive industry: Current status and perspectives, *Mater.Sci.Eng.B*, 2009, 161, 182-187.

[3] Manicone FP.F., Iommetti P.R., Raffaelli L.: An overview of zirconia ceramics: Basic properties and clinical applications, *J.of Dentistry*, 2007, 35, 819-826.

[4] Krell A., Hutzler T., Klimke J. : Transmission physics and consequences for materials selection, manufacturing, and applications, *J.Eur.Ceram.Soc.*, 2009, 29, 207-221.

[5] Wiederhorn S.M.: Subcritical crack growth in ceramics, in *Fracture Mechanics of Ceramics*, v.2 ed. By Bradt R.C., Hasselman D.P.H., Lange F.F., Plenum Press, New York, London, 1974, 613-646.

[6] Konopka K., Maj M., Kurzydłowski J.K.: Studies of the effect of metal particles on the fracture toughness of ceramic matrix composites, *Materials Characterization*, 2003, 51, 5, December, 335-340.

[7] Ostertag C.P.: Influence of fiber and grain bridging on crack profiles in SiC fiber-reinforced alumina-matrix composites, *Mater.Sci.Eng. A*, 1999, 260, 124-131.

[8] Bocanegra-Bernal M.H., Echeberia J., Ollo J.,et al.: A comparison of the effects of multi-wall and single--wall carbon nanotube additions on the properties of zirconia toughened alumina composites, *Carbon*, 2011, 49, 5, 1599-1607.

[9] Boniecki M., Gołębiewski P., Wesołowski W., et al.: Alumina/zirconia composites toughened by the addition of graphene flakes, *Ceram. Int.*, 2017, 43, 10066-10070.

[10] Liu J., Yan H., Reece M.J., Jiang K.: Toughening of zirconia/alumina composites by the addition of graphene platelets, *J.Eur.Ceram.Soc.*, 2012, 32, 4185-4193.

[11] Shin J-H., Hong S-H.: Fabrication and properties of reduced graphene oxide reinforced yttria-stabilized zirconia composite ceramics, *J.Eur.Ceram.Soc.*, 2014, 34, 1297-1302.

[12] Fei Ch., Jin D., Tyeb K., et al.: Field assisted sintering of graphene reinforced zirconia ceramics, *Ceram.Int.*, 2015, 41, 6113-6116.

[13] Li J-F., Watanabe R.: Fracture toughness of Al_2O_3 - particle-dispersed Y_2O_3 - partially stabilized zirconia, *J.Am.Ceram.Soc.*, 1995, 78, 1079-1082.

[14] Lee J-K., Kim M-J., Lee E-G.: Influence of dispersed--alumina particle size on the fracture toughness of 3 mol% yttria-stabilized zirconia polycrystals (3Y-TZP), *J.Mater.Sci.Lett.*, 2002, 21, 259-261.

[15] Vleugels J., Van der Biest O.: Development and characterization of Y_2O_3 – stabilized ZrO_2 (Y-TZP) composites with TiB_2, TiN, TiC, and $TiC_{0.5}N_{0.5}$, *J.Am. Ceram.Soc.*, 1999, 82 [10] 2717 – 2720.

[16] Basu B., Vleugels J., Van der Biest O.: Processing and mechanical properties of ZrO_2 – TiB_2 composites, *J.Eur.Ceram.Soc.*, 2005, 25, 3629-3637.

[17] Haberko K., Pędzich Z. Róg G., Bućko M.M., Faryna M.: The TZP matrix-WC particulate composites, *Eur.J.Solid State Inorg. Chem.*, 1995, 32, 593-601.

[18] Pędzich Z., Haberko K.: Toughening mechanism in the TZP - WC particulate composites, *Key Eng.Mater.*, 1997, 132-136, 2076-2079.

[19] Pędzich Z., Haberko K., Piekarczyk J., Faryna M., Lityńska L.: Zirconia matrix-tungsten carbide particulate composites manufactured by hot-pressing technique, *Mater. Lett.*, 1998, 70-75.

[20] Pędzich Z.: The reliability of particulate composites in the TZP/WC system, *J.Eur.Ceram.Soc.*, 2004, 24, 3427-3430.

[21] Pędzich Z.: Fracture of oxide matrix composites with different phase arrangement, *Key Eng. Mater.*, 2009, 409, 244-251.

[22] Pędzich Z.: Tungsten Carbide as an reinforcement in structural oxide-matrix composites, *INTECH open science/open minds, chapter 4 (Tungsten Carbide - Processing and Applications)*, (2012), 81-102, (http://dx.doi.org/10.5772/51183).

[23] Űnal N., Kern F., Ővecoglu M.L., Gadow R.: Influence of WC particles on the microstructural and mechanical properties of 3 mol % Y_2O_3 stabilized ZrO2 matrix composites produced by hot pressing, *J.Eur.Ceram.Soc.*, 2011, 31, 2267- 2275.

[24] Bamba N., Choa Y-Ho, Sekino T., Niihara K.: Mechanical properties and microstructure for 3 mol% yttria doped zirconia/silicon carbide nanocomposites, *J.Eur.Ceram.Soc.*, 2003, 23, 773-780.

[25] Zhan G.-D., Lai T.-R., Shi J.-L., Yen T.-S., Zhou Y. Zhang Y.: Microstructure and mechanical properties of yttria-stabilized tetragonal zirconia polycrystals containing dispersed TiC particles, *J.Mater.Sci.*, 1996, 31, 2903-2907.

[26] Stevens R.: Zirconia and zirconia ceramics. Introduction to zirconia. Magnesium Electron Publication. 113, July (1986), 56 pages.

[27] Cutler R.A., Reynolds J.R., Jones A.: Sintering and characterization of polycrystalline monoclinic, tetragonal and cubic zirconia, *J.Am.Ceram.Soc.*, 1992, 73[8], 2173-2183.

[28] Govila R.K.: Strength characterization of yttria--partially stabilized zirconia, *J.Mater.Sci.*, 1995, 30, 2656-2667.

[29] Anstis G.R, Chantikul P., Lawn B.R., Marchall D.B.: A critical evaluation of indentation techniques for fracture toughness, *J.Am.Ceram.Soc.*, 1981, 64, 533-538.

[30] Niihara K.: A fracture mechanics analysis of indentation-induced Palmqvist crack in ceramics, *J.Mater. Sci. Lett.*, 1983, 2, 221-223.

[31] Boniecki M.: unpublished data, 2018.

[32] Bozkurt F., Schmidova E.: Fracture toughness evaluation of S355 steel using circumferentialy notched round bars, *Periodica Polytechnica Transportation Engineering*, 2018, 1-5, https://doi.org/10.3311/PPtr.11560.

[33] Munro R.G.: Evaluated material properties for a sintered α – alumina, *J.Am.Ceram.Soc.*, 1997, 80 (8), 1919-1928.

[34] https://accuratus.com/silicar.html.

[35] Vallauri D., Adrian I.C.A., Chrysanthou A.: TiC – TiB2 composites: A review of phase relationships, processing and properties, *J. Eur.Ceram. Soc.*, 2008, 28, 1697 – 1713.

[36] Małek O., Lauwers B., Perez Y., De Baets P., Vleugels J.: Processing of ultrafine ZrO_2 toughened WC composites, *J.Eur. Ceram.Soc.*, 2009, 29, 3371-3378.

[37] Selsing J.: Internal stresses in ceramics, *J.Am.Ceram. Soc.*, 1961, 44,419.

[38] Budiansky B., Hutchinson J.W., Lambropoulus J.C.: Continuum theory of dilatant transformation toughening in ceramics, *Int.J.Solids Struct.*, 1983, 19, 337-355.

[39] Evans A.G., Cannon R.M.: Toughening of brittle solids by martensitic transformation, *Acta Metall.*, 986, 34, 761-800.

[40] PN-EN ISO 15732, October 2007. Fine ceramics (advanced ceramics, advanced technical ceramics). Test method for fracture thoughness of monolithic ceramics at room temperature by single edge precracked beam (SEPB) method (ISO 15732:2003) (Eq. 8).

[41] Chantikul P., Anstis G.R., Lawn B.R, Marshall D.B.: A critical evaluation of indentation techniques for measuring fracture toughness: II, Strength method, *J.Am.Ceram.Soc.*, 1981, 64 [9], 539-543.

[42] PN – EN 843-1, December 2007. Advanced technical ceramics - Monolithic ceramics - Mechanical properties at room temperature - Part 1: Determination of flexural strength.

[43] PN-EN 843-2, December 2007. Advanced technical ceramics - Monolithic ceramics - Mechanical properties at room temperature - Part 2: Determination of the Young's modulus, shear modulus and Poisson's ratio.

[44] Boniecki M., Gołębiewski P., Wesołowski W. i inni: Kompozyt Al_2O_3-ZrO_2 wzmocniony płatkami grafenowymi/Al_2O_3-ZrO_2 composite reinforced with graphene platelets, *Materiały Elektroniczne/Electronic Materials*, 2016, 44, 1, 20-28.

Electric measurements

The Department of Composites and Ceramic Materials

SeebTest 1.0 producent PESS

Facilities:

Simultaneous determination of Seebeck Coefficient and Electrical Conductivity. Electrical conductivity and Seebeck coefficient (thermoelectric properties) of semiconductor and metallic materials can be characterized in a single measurement with the 4-probe method in vacuum or inert protective atmosphere. A sample is vertically placed between current electrodes (two-heater system) and compressed by 5N force. The Peltier effect is minimized by using an alternated current.

Sample size:

- Cylindrical (from 5.0 to 13.0 mm, length 6-20mm)
- Rectangular (from 5.0x5.0 to 10.0x10.0 mm, length 6-20mm)
- Other shapes are also possible after consultation

Parameters:

- Temperature range: RT - 550°C with unlimited number of temperature steps
- Seebeck Coefficient range: 5 – 1000 μV/K with accuracy better than 5%
- Electrical conductivity range: 0.1 – 1000000 S/m with accuracy better than 5%
- Atmosphere: vacuum 10 $^{-3}$ mbar, inert, oxidizing

RESEARCH NETWORK ŁUKASIEWICZ

Insitute of Electronic Materials Technology

Wólczyńska 133,
01-919 Warszawa

+48 22 835 30 41
+48 22 639 58 05

itme@itme.edu.pl
komercjalizacja@itme.edu.pl

Porous volumetric structures obtained by additive manufacturing technologies

Kamil Kaszyca[1], Wojciech Danilczuk[2], Rafał Zybała[1,3]

The goal of our work was to develop bulk structures characterized by a variable, controlled porosity, using additive manufacturing techniques (3D printing). A technology for the fabrication of bulk materials with controllable porosity has been developed. For that purpose, the samples with constant porosity were designed and then prepared, which allowed us to learn the possible limit values. Thus, we were able to optimize the design process at the stage of the preparation of the gradient structures.

Key words: 3D printing, porous materials, gradient materials, design of porous structures

Porowate struktury przestrzenne otrzymywane technikami wytwarzania przyrostowego

Niniejsza praca przedstawia proces opracowanie struktur przestrzennych charakteryzujących się zmienną, sterowaną porowatością, z wykorzystaniem technik wytwarzania przyrostowego (druku 3D). W ramach pracy opracowana została technologia wytwarzania materiałów o sterowanej porowatości. W tym celu zaprojektowane i wykonane zostały próbki o stałej porowatości. Pozwoliło to na poznanie możliwych do uzyskania wartości granicznych, co w konsekwencji skutkowało możliwością optymalizacji procesu projektowania na etapie tworzenia struktur gradientowych.

Słowa kluczowe: druk 3D, materiały porowate, materiały gradientowe, projektowanie struktur porowatych

DOI: https://doi.org/10.34769/tmjb-1g07

1. Introduction

Additive manufacturing techniques are at the center of interest for many research groups. For instance, the authors of the recent report [1] mention a prediction that in the years 2016-2020 the market value of 3D printing will increase from 6.1 billion dollars to 21 billion dollars. The article describes the examples of the applications of numerous common techniques, including fused deposition modelling, inkjet printing, stereolithography and selective laser melting/sintering. The possibilities of the use of these techniques for processing of a variety of materials were presented, i.e. polymers (PLA, ABS, resins), metals (Ti-Al-V), ceramic, concrete and composites. Due to the fact that the additive manufacturing techniques can be easily adapted to various purposes and the ability to rapidly obtain customized parts, these methods have a ide range of applications, not only for the production of mechanical elements. The possibility of using electrically conductive polymers enables printing of functional components of the electronic devices, eventually serving as e.g. integrated printed circuit boards [2]. The materials with a variable porosity can be applied as the intermediate products to be used for the production of porous ceramics. They may be intended for metal infiltration or utilized as filters, bone implants [3] or the substrates to be applied in bionics [4, 5]. The composites with a polymer matrix [6] are also used in bionics or in the aircraft industry. The real advantage of the proposed method is that the user has the possibility to obtain a part with a well-defined, customized geometry and structure [7-9], and with high specific strength [10]. Today, a dynamic development of the additive manufacturing techniques is related to a steady increase in their popularity and accessibility. The results of the preliminary studies, presented below, contribute to the growth of the methodology enabling the application of the additive manufacturing techniques for the fabrication of the functionally gradient materials.

The goal of our research was to elaborate a technology to produce the plastics with a controlled open porosity.

[1] *Łukasiewicz Research Network - Institute of Electronic Materials Technology*, 133 Wólczyńska Str., 01-919 Warsaw, Poland e-mail: kaszyca@itme.edu.pl
[2] *Lublin University of Technology, Faculty of Mechanical Engineering, Department of Automation*, Nadbystrzycka 36, 20-618 Lublin, e-mail: wojciech.danilczuk@pollub.edu.pl
[3] *University Research Centre "Functional Materials", Warsaw University of Technology*, Wołoska 141, 02-507 Warsaw, Poland; e-mail: rafal.zybala@pw.edu.pl

At the stage of the design of experiments, the following assumptions were made:

1. The scientific and technological work will enable obtaining a material with an assumed porous structure

2. The control of the process parameters makes it possible to obtain a structure with a gradient porosity

3. A porosity limit value exists that allows open porosity to be obtained.

The article presents the results of the technological and research work carried out in the framework of the project "Porous spatial structures obtained by additive manufacturing techniques", performed at the Institute of Electronic Materials Technology (ITME) as a part of the statutory work. The fabrication of a plastic part with a gradient porosity was considered a criterion for the success of the project. The materials described here were manufactured with a device utilizing the FDM Wanhao Duplicator i4. The material chosen for the tests was Polyactide, made by the Polish company Propox, characterized by a negligible shrinkage during cooling. The batch files for the apparatus were prepared using the IceSl slicer.

2. Methodology for materials fabrication by FDM technique

The materials described in our article have been obtained by the FDM (fused deposition modeling) method, which consists in the formation of a part by a proper deposition of the layers of a plasticized thermoplastic material. After the deposition of each layer, the working platform with the piece being printed moves away from the print head by a distance equal to the thickness of the deposited layer. The devices operating with the use of the FDM technique utilize polymers and their composites as the building materials.

The main parameters responsible for the thickness and density of the filling of a solid are: a factor called INFILL and the layer height (L_h). Additionally, the most important technological parameters are: V - the nozzle linear velocity, T_h - the nozzle temperature and T_b - the substrate temperature. Figure 1 shows the dependence of the planar fill on the INFILL parameter for a single layer (a, b, c) and for two layers (d, e, f).

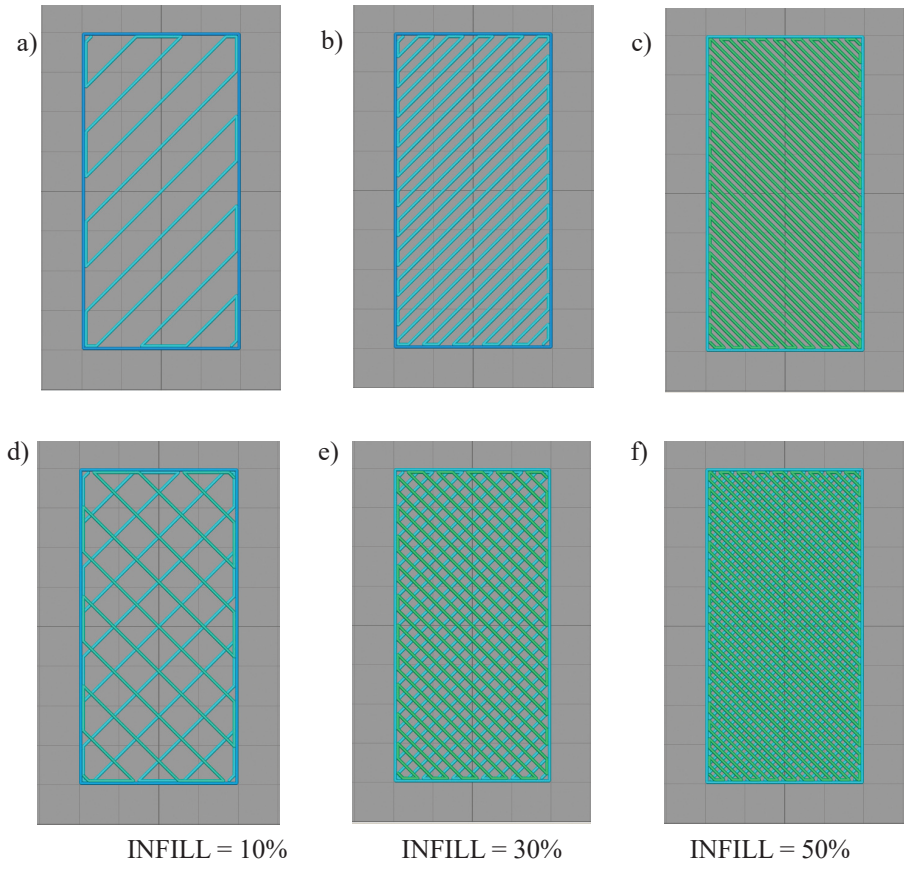

Fig. 1. The planar fill - INFILL factor dependence.
Rys. 1. Zależność wypełnienia od współczynnika INFILL.

As demonstrated on the model example, it is still possible to obtain a structure with open porosity even in the case of 50% filling. The model-based predictions indicated that with the perfect reproduction of the expected layer, any value of INFILL less than 100% would not lead to closed porosity. Due to the discrepancies between the model and the real data, as well as because of the practical aspect of our investigations, later in the report we will focus on the description of the actual conditions and the presented information will be based on the experimental results.

3. Experimental

The goal of the studies reported in this article was the production of a part with a continuously graded porosity. In the described work a series of the samples was made for the following purposes:

1) The examination of the effect of the deposited layer height on the size and the contribution of the pores
(from sample TEST-01 to sample TEST-05)

2) The examination of the effect of the INFILL value on the size and the contribution of the pores
(from sample TEST-01 to sample TEST-05)

3) Preliminary searching for the limit INFILL values that could allow open porosity to be obtained
(from sample TEST-06 to sample TEST-15)

4) The examination of the dependence between the INFILL value and the planar void fraction of the porous zone
(from sample TEST-06 to sample TEST-15)

5) Detailed searching for the limit INFILL values allowing open porosity to be obtained (a series of test samples with discontinuously graded porosity)

Table 1 shows a list of samples prepared during the first stage of the investigations. The tests were performed in order to verify a relationship between the chosen parameters of printing (L_h, INFILL) and the geometry of the pores of the obtained sample, as well as to find the limiting process parameters corresponding to open porosity. The test samples produced at this stage of work had a form of a rectangular prism with the dimensions of 20 × 10 × 10 mm.

Tab. 1. A list of the investigated samples.
Tab. 1. Lista próbek do badań.

ID	Material	Conditions					Substrate
		T_h[°C]	T_b[°C]	L_h[°C]	INFILL	V [m/s]	
TEST-01	PLA	195	65	0.15	50%	0.037	Glass plate „Float", thickness 4 mm
TEST-02	PLA	195	65	0.2	40%		
TEST-03	PLA	195	65	0.2	50%		
TEST-04	PLA	195	65	0.2	60%		
TEST-05	PLA	195	65	0.25	50%		
TEST-06	PLA	195	65	0.2	10%		
TEST-07	PLA	195	65	0.2	20%		
TEST-08	PLA	195	65	0.2	30%		
TEST-09	PLA	195	65	0.2	40%		
TEST-10	PLA	195	65	0.2	50%		
TEST-11	PLA	195	65	0.2	60%		
TEST-12	PLA	195	65	0.2	70%		
TEST-13	PLA	195	65	0.2	80%		
TEST-14	PLA	195	65	0.2	90%		
TEST-15	PLA	195	65	0.2	100%		

T_h - the nozzle temperature, T_b - the substrate temperature, L_h - the layer height, INFILL - the infill factor, V - the nozzle velocity

3.1. Pore geometry analysis

Pore geometry analysis was based on a series of test samples TEST-01-TEST-15. The presented structures are oriented in the XY plane of the printer on a glass substrate. At this stage of research, the influence of two parameters on the geometry of pores in the resulting material was examined. The study of pore geometry was based on the analysis of the cross-sectional photographs of the produced materials.

Figure 2 shows the photographs of the analyzed samples listed in Table 1.

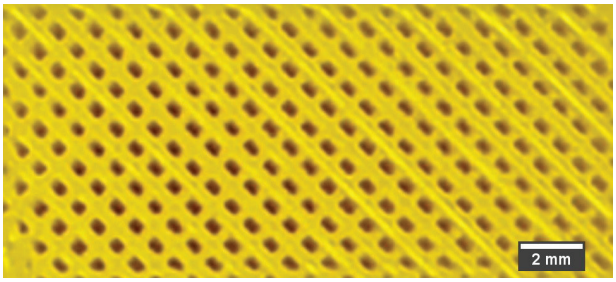

a) TEST-1

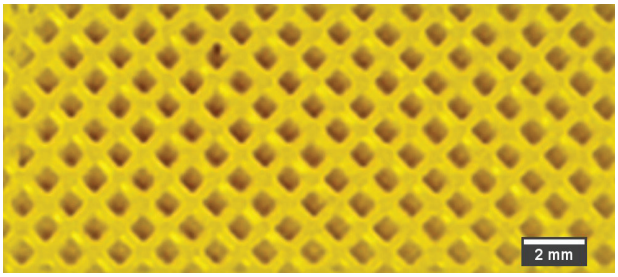

b) TEST-2

c) TEST-3

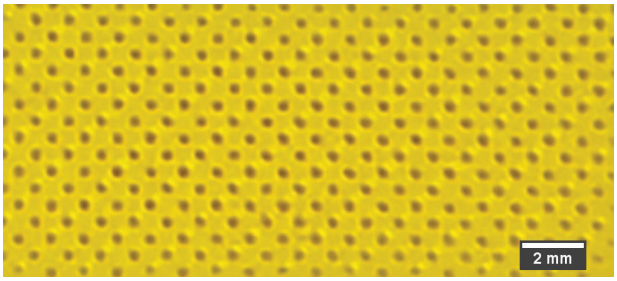

d) TEST-4

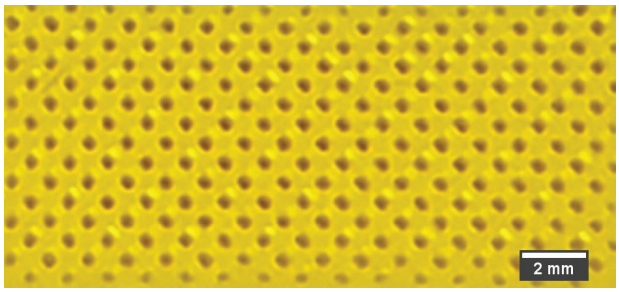

e) TEST-5

Fig. 2. Photographs of the surface of the analyzed samples.
Rys. 2. Fotografie powierzchni analizowanych próbek.

On the basis of the photographs, a binary mask was prepared, where the white region represented the presence of a polymer and a black region indicated the lack of a polymer. The histogram of the mask enabled the determination of the material porosity, while the analysis of the particles provided information on the average pore size ($A_{śr}$). Further steps of an exemplary process of the image analysis are presented in Figure 3. The analysis results are collected in Table 2. For the image analysis an ImageJ software was used.

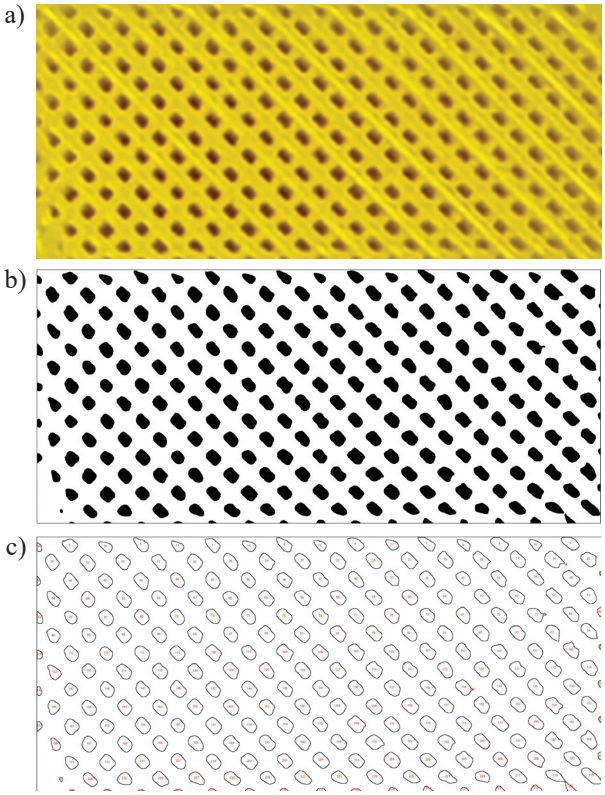

Fig. 3. The stages of PSD analysis.
Rys. 3. Poszczególne etapy analizy obrazu.

Tab. 2. The results of image analysis.
Tab. 2. Wyniki analizy obrazu.

Sample ID	L_{height} [mm]	Infill	Sum [px]	White region [px]	Black region [px]	Number of pores [-]	Average pore size [px]	Average pore size [mm²]	Planar void fraction [%]
TEST-1	0.15	50%	1300328	994661	305667	246	162.69	0.155	23.5
TEST-2	0.2	40%	1255464	865857	389607	159	157.1	0.307	31.0
TEST-3	0.2	50%	1255616	981092	274524	225	157.1	0.153	21.9
TEST-4	0.2	60%	1209632	999178	210454	323	151.3	0.082	17.4
TEST-5	0.25	50%	1298772	1053066	245706	240	162.5	0.128	18.9

In order to examine the relationship between the values of INFILL and the planar void fraction for the material, an image analysis was performed for the series of samples from TEST-6 to TEST-15. The results of the analysis of the structures are presented in Figure 4. It can be seen that the planar void fraction of the porous structure formed depends in a nonlinear manner on the values of INFILL.

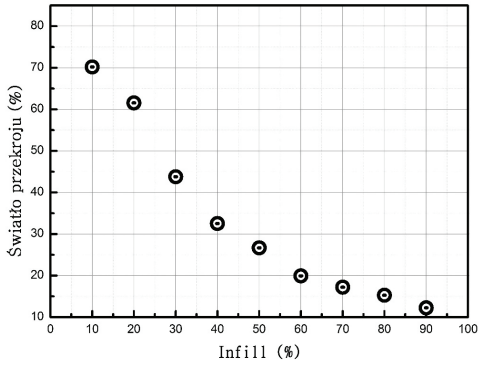

Fig. 4. The planar void fraction - INFILL factor dependence.
Rys. 4. Zależność pomiędzy światłem przekroju a współczynnikiem INFILL.

Analysis of the boundary conditions that allow open porosity to occur

A starting point of our study was the determination of the filling limit value that can ensure the existence of open porosity. For this purpose, a series of test samples with different INFILL values was made. Figure 5 shows an exemplary photograph of a cross-section of a test sample made of 12 zones with the consecutive INFILL values equal to 10%, 15%, ... 70%. The presented structure was obtained by cutting the test sample with a diamond saw in the ZX plane and then grinding the uncovered plane to remove the material exposed to a deformation as a result of cutting.

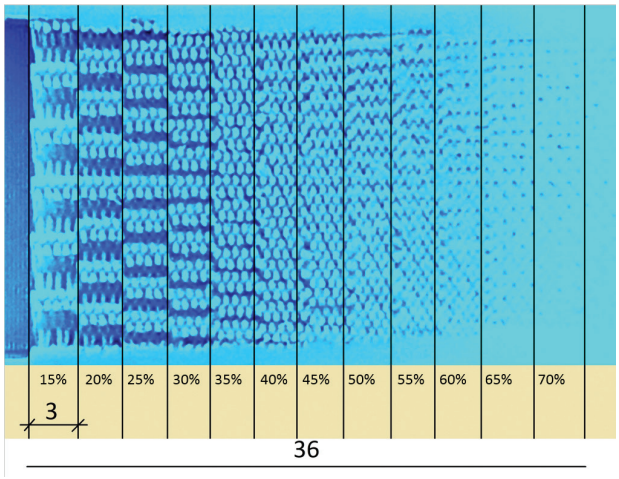

Fig. 5. A photograph of a cross-section of an exemplary test sample.
Rys. 5. Fotografia przekroju przykładowego testera.

To verify permeability of the layers, a series of test samples was prepared with INFILL values ranging from 60% to 90% at the intervals of 5%. It was determined experimentally that the limit value of the layer permeability for gases was 85%. However, a significant increase in the flow resistance was observed already at 70% filling.

Fabrication of an open-graded porous part

On the basis of the data obtained at the stage of the analysis of the samples from the TEST-XX series and the test samples with discontinuously graded porosity, a model of a gradient material has been developed. The elaborated model was a 25 × 50 × 30 mm rectangular prism with a gradient value of INFILL, ranging from 10% to 60%. The values of the planar void fraction of that material varied between 76% and 17%. Figure 6 shows a photograph of a cross-section of the aforementioned gradient material.

The obtained results make it possible to design a structure with a controllable porosity, previously determined at

the stage of the porosity design. The desired nature of the porosity changes can be arbitrary (within the technical possibilities of the FDM method).

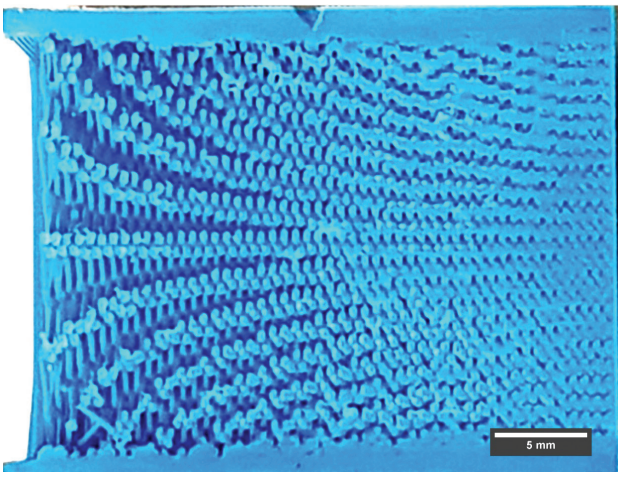

Fig. 6. A photograph of a cross-section of a gradient material.
Rys. 6. Fotografia przekroju otrzymanego detalu o gradientowo zmieniającej się porowatości.

The elaborated technology enables formation of a part with any kind of geometry and with a porosity gradient changing along one of the axes of the part. It is possible to utilize the obtained results for the production of ceramic foams. According to the proposed methodology, a porous structure would be filled with a ceramic material and then the matrix would be removed by its thermal decomposition. A prefabricated product formed in that way, subjected to free sintering process, would be brought to the form of a polycrystalline ceramic material with open porosity. Potentially, the aforementioned products can also find an application as filters. It is possible to use a polymer with silver or titanium oxide particles, which after their activation by UV radiation may purify the flowing fluid from the microorganisms.

4. Conclusions

The results reported here indicate the possibility of utilizing a popular method of additive manufacturing for the production of porous materials. Our article also presents a methodology for optimizing the printing parameters. Figure 7 shows photographs of the exemplary structures.

The use of additive manufacturing techniques to produce gradient materials is a novel idea. Our paper describes the preliminary studies on the applicability of the FDM technique for the fabrication of porous materials. Further work will be focused on the extending of the range of materials by including metals and ceramics, as well as on functionalization of the obtained structures. The analysis of the experimental results has revealed the following relationships:

1. It has been established that the limit value of the INFILL coefficient is 65%, which allowes for a free transport of fluids and powders.

2. With an increase in the layer height L_h at a constant value of INFILL factor, the values of both average pore size and planar void fraction of the structure decrease, whereas the number of pores increases.

3. An increase in the value of the INFILL factor results in an increase in the number of pores and a decrease in both the average pore size and the planar void fraction of the structure.

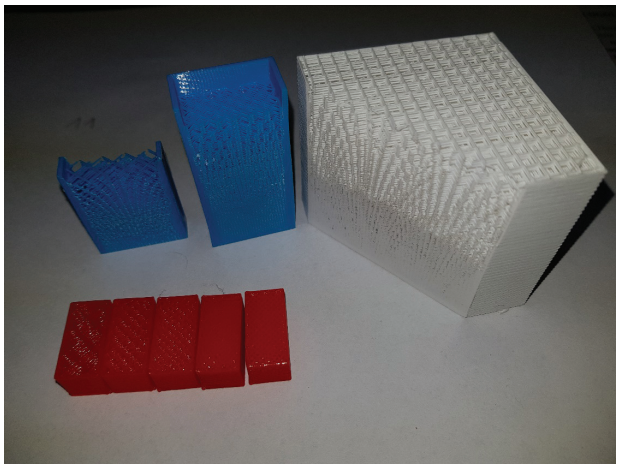

Fig. 7. A photograph of the exemplary structures.
Rys. 7. Fotografia przykładowych struktur.

References

[1] Ngo T.D., Kashani A., Imbalzano G., Nguyen K.T.Q., and Hui D.: Additive manufacturing (3D printing): A review of materials, methods, applications and challenges, *Compos. Part B Eng.*, vol. 143, no. June, pp. 172–196, 2018.

[2] Gnanasekaran K. et al.: 3D printing of CNT - and graphene-based conductive polymer nanocomposites by fused deposition modeling, *Appl. Mater. Today*, vol. 9, pp. 21–28, 2017.

[3] Hwa L.C., Rajoo S., Noor A.M., Ahmad N., and Uday M.B.: Recent advances in 3D printing of porous ceramics: A review, *Curr. Opin. Solid State Mater. Sci.*, vol. 21, no. 6, pp. 323–347, 2017.

[4] Fee C.: 3D-printed porous bed structures, *Curr. Opin. Chem. Eng.*, vol. 18, pp. 10–15, 2017.

[5] Jakus A.E., Geisendorfer N. R., Lewis P.L., and Shah R.N.: 3D-printing porosity: A new approach to creating elevated porosity materials and structures, *Acta Biomater.*, vol. 72, pp. 94–109, 2018.

[6] Wang X., Jiang M., Zhou Z., Gou J., and Hui D.: 3D printing of polymer matrix composites: A review and prospective, *Compos. Part B Eng.*, vol. 110, pp. 42–458, 2017.

[7] Fee C., Nawada S., and Dimartino S.: 3D printed porous media columns with fine control of column packing morphology, *J. Chromatogr. A*, vol. 1333, pp. 18–24, 2014.

[8] Fousová M., Vojtěch D., Kubásek J., Jablonská, E. and Fojt J.: Promising characteristics of gradient porosity Ti-6Al-4V alloy prepared by SLM process, *J. Mech. Behav. Biomed. Mater.*, vol. 69, no. October 2016, pp. 368–376, 2017.

[9] Nawada S., Dimartino S., and Fee C.: Dispersion behavior of 3D-printed columns with homogeneous microstructures comprising differing element shapes, *Chem. Eng. Sci.*, vol. 164, pp. 90–98, 2017.

[10] Dizon J.R.C., Espera A.H., Chen Q., and Advincula R.C.: Mechanical characterization of 3D-printed polymers, *Addit. Manuf.*, vol. 20, pp. 44–67, 2018.

Dilatometric measurements

The Department of Composites and Ceramic Materials

DIL 402 Expedis NETZSCH

Facilities:

- Dilatometer DIL 402 Select Expedis allows to analysis of length change phenomena of different materials (metals, ceramics, polymers, composites), thus revealing information regarding their behavior during heating or cooling process.
- For preparing a measurement, the defined sample is inserted into a holder and brought into contact with the pushrod. After closing the furnace the temperature rises and the linear thermal expansion can be measured. Thermal expansion of the sample during heating is detected by the displacement system.
- System allows for detection of phase transitions, density change, shrinkage steps, sintering behavior, etc.

Parameters:

- Temperature range: RT - 1100°C
- Measuring range: ±25 mm
- Pushrod load: 0.01- 3.0N
- Atmosphere: Argon

Sample size:

- Rectangular (from 3.0x3.0 to 8.0x8.0 mm, length 12-25mm)
- Cylindrical (from 3.0 to 10.0 mm, length 12-25mm)

RESEARCH NETWORK ŁUKASIEWICZ

Insitute of Electronic Materials Technology

Wólczyńska 133,
01-919 Warszawa

+48 22 835 30 41
+48 22 639 58 05

itme@itme.edu.pl
komercjalizacja@itme.edu.pl

40 years of the Institute of Electronic Materials Technology

Patrycja Skoczek[1], Szymon Plasota[1]

DOI: https://doi.org/10.34769/fas4-vb25

THE ORIGIN OF ITME

The origin of the Institute of Electronic Materials Technology (ITME) dates back to the 1970s. In 1970 the Scientific-Production Center of Semiconductors CEMI (NPCP) came into being. Comprising the TEWA Semiconductor Factory, the Institute of Electron Technology and the Industrial Institute of Electronics.

On 1 July 1970 the Scientific and Production Center of Semiconductor Materials (ONPMP) was established in Warsaw, acting as a branch of the Scientific-Production Center of Semiconductors. The person who initiated of the foundation of the center was prof. Bolesław Jakowlew, who also became its first director. Established in the NPCP by The Minister of Machine Industry the Experimental Department of Semiconductor Materials Manufacturing to prepare for the production and the experimental production of materials such as semiconductor materials, high-purity metals and chemical compounds as well as ceramics and glass. In the following year, the Experimental Department was incorporated to the Scientific and Production Center of Semiconductor Materials.

The main activity of the Scientific and Production Center of Semiconducting Materials was to solve the problems concerning materials by undertaking the tasks such as conducting both fundamental and applied research, development and implementation work as well as by carrying out the production at the Experimental Department.

The areas of the activity of the Center included the development of technology and the research concerning the following materials:

- silicon and germanium,
- semiconductor compounds of the $A^{III}B^{V}$ and $A^{II}B^{VI}$ type
- high-purity metals and special-purpose alloys,
- chemical compounds applied in the production of semiconductor devices and microelectronic systems,
- dielectrics and products made of these materials,
- openworks for integrated circuits.

Fot. Maciej Żyliński

The year 1973 marked the start of the quarterly bulletin "Electronic Materials" with prof. Bolesław Jakowlew as its first editor-in-chief. The bulletin has been issued ever since.

[1] *Łukasiewicz Research Network - Institute of Electronic Materials Technology*, 133 Wólczyńska Str., 01-919 Warsaw, Poland e-mail: patrycja.skoczek@itme.edu.pl

In the years 1970-1975 the Scientific and Production Center of Semiconductor Materials started the production of over three hundred ranges of special purpose materials. Thanks to the very good results achieved in the field of materials, ONPMP was voted a leading role in the Government Research and Development Program PR-3 "Materials and components for electronics". The main task of the research center was to coordinate the research projects and the implementation of the new materials, in various the institutions of several departments.

In 1978 the Experimental Department of Semiconductor Materials Manufacturing was selected from ONPMP, to form a state-controlled enterprise, named the Electronic Materials Scientific and Production Centre (CNPME).

THE ESTABLISHMENT OF ITME

The Institute of the Electronic Materials Technology was established after transformation of the Scientific and Production Center of Semiconductor Materials by the Ordinance no 14 of the Prime Minister of 5 February 1979 (the Official Journal of the Republic of Poland "Monitor Polski", M.P, No. 4, Item 37). The Institute was controlled by the Minister of Machine Industry and directed by the Director of the Electronic Materials Scientific and Production Centre. The Institute carried out the research and development projects, and dealt with the implementations in the field of electronic materials. In particular, their work concetrated on the technology of obtaining, processing and the effective applications of the materials to the needs of electronization.

In the years 1982-1983 the production processes were transferred to new premises, located at Wólczyńska Street 133 in Warsaw. The first director of the Institute (until 1980) was prof. Bolesław Jakowlew. In the consecutive years Mieczysław Frącki, Ph.D. (in the years 1980-1987), followed by Wiesław Marciniak, Ph.D., D.Sc., Prof. (1987-1994). Took over the post in February 1994 as a result of public competition Zygmunt Łuczyński, Ph.D., was appointed director of the Institute through a public competition.

RESEARCH INSTITUTE AND ŁUKASIEWICZ RESEARCH NETWORK

On 1 October 2010 pursuant to the Act on Research Institutes of 30 April 2010 (Journal of Laws [Dz. U.] No. 96/2010, Item 618), the legal form of the Institute of Electronic Materials Technology was changed transforming it into a research institute under the supervision of the Minister of Economy.

In 2015 Ireneusz Marciniak, Ph.D., won the competition for the post of the director of the Institute. In 2016 the following divisions were included in the organizational structure of the scientific departments compromised the following divisions: Department of High Purity Materials Characterization, Department of Microstructural Research, Department of Ceramic-Metal Composites and Joints, Department of Ceramics, Department of Silicon Technology, Department of Optoelectronics, Department of Chemical Technologies, Laboratory of Mössbauer Spectroscopy, Department of Glass, Department of Epitaxy, Department of Epitaxy and Characterization, Department of Thick-Film Materials, Department of Functional Materials, Department for Applications of $A^{III}B^{V}$ Materials and Department of Piezoelectronics.

In 2017 Zbigniew Matyjas, Ph.D., D.Sc., was appointed the new director of the Institute. The restructuring that was then initiated has brought many changes and has been continued until prezent day.

On 1 April 2019, ITME became one of 38 institutes of the Łukasiewicz Research Network, and its name was changed to the Łukasiewicz Research Network - Institute of Electronic Materials Technology. The Łukasiewicz Research Network, established under the Act of 21 February 2019, is providing complete business solutions within 6 research groups: automation, chemistry, biomedicine, teleinformatics, materials and production. The Institute belongs to the group named “materials”.

RESEARCH DEPARTMENTS OF ŁUKASIEWICZ - ITME

There are several scientific-research departments operating in ŁUKASIEWICZ - ITME, together with the separate Laboratory of Structural Research and Materials Characterization and the Electron-beam and nanoimprint laboratory.

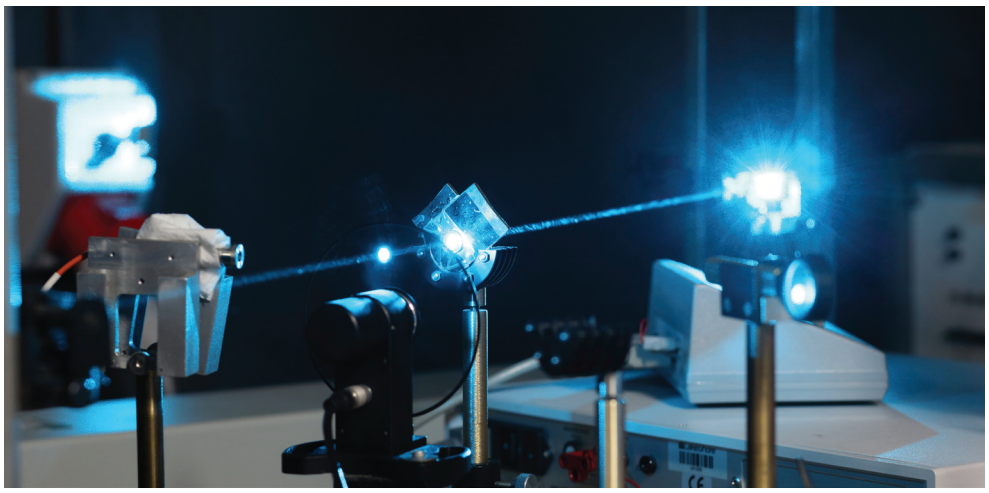

The activity of the Department of Graphene and Materials for Electronics is focused on the investigations of the epitaxial structures of the compounds of III--V and I-IV semiconductors for electronic applications as well as on the manufacture of high-quality graphene on SiC, Ge and metallic substrates. The technologies of semiconductor devices on the single-crystal matrices and epitaxial layers are also developed. Our professional technological equipment enables the structures based on GaAs, InP, GaN, GaSb and SiC to be produced with the highest quality, using the chemical vapor deposition method (CVD and MOCVD).

The Department of Chemical Synthesis and Graphene Flakes specializes in the chemical synthesis of advanced materials, designed to be utilized in materials science and engineering, electronics, optoelectronics and in the energy production and storage industry. The team that works in that department has extensive experience in the manufacture of nanomaterials, including graphene flakes. The most intensive studies concern the applications of the chemical methods to obtain graphene flakes and their derivatives, as well as the composite materials containing graphene structures. Simultaneously, the research is carried out on the chemical synthesis of the nanocrystalline materials and nanostructures, performed with various techniques, namely: sol-gel process, co-precipitation, hydrothermal synthesis, combustion synthesis, reversed microemulsion synthesis, electrochemical method and the solid phase methods, including microwave synthesis and mechanosynthesis. The third area of the scientific interests of the Department concerns the synthesis of electrode materials for lithium-ion cells and supercapacitors.

The Department of Composite and Ceramic Materials specializes in the manufacture of ceramic-metal composite materials, graded materials and welding advanced materials. In particular, the physical and chemical phenomena, accompanying the aforementioned processes, are also considered. The following examples of composite materials are obtained: materials with high thermal conductivity, contact materials and construction materials. The scientists work on the preparation and characterization of the thermoelectric materials designed for energy conversion. The investigations are focused on two groups of materials - skutterudites and tellurides (of antimony and bismuth). The composite materials are manufactured using powder metallurgy or by the infiltration of porous ceramic preforms with a liquid alloy. The Department is also responsible for developing technologies of welding composite materials with other types of materials, including combining various electrical insulators (corundum, nitride ceramics, carbide ceramics, glass) with metals (copper, molybdenum, FeNi alloys, steels) for the vacuum, electronic and nuclear applications as well as to the use in power engineering.

The research carried out at the Department of Optoelectronics covers a wide range of subjects: development of new sources of white light, laser diodes, solid-state lasers, heat removal techniques, assembly and integration of optoelectronic devices, as well as optical and thermal characterization of various materials and devices. Thanks to their long-term experience, the scientists working in that department have managed to develop a numerous innovative devices, such as: low-beam divergence high--power laser diodes characterized, with optical fiber lead or devices integrated with diffractive optical components, installed on microchannel coolers. The scientists offer new solutions in the dedicated laser sources, the integration and assembly of the electronic devices. We provide services in the design of the prototypes of optoelectronic devices, as well as in testing of the materials for photonics.

The team of the Department of Glass has extensive experience in manufacturing optical-fiber components, image guides and classic optical waveguides (including active fibers) and photonic crystal fibers (passive and active), as well as nano-optic components. By combining the technological capacities with the fiber design and computer modelling abilities, our scientists can match the customer's requirements in the production of micro- and nanostructured optical fibers and fiber optic components for the range of the visible, near infrared and middle infrared radiation. The application areas concern nonlinear optics (supercontinuum generation), polarization wavefront shaping and the introduction of the light beam into the micro-optofluidic systems.

The Department of Experimental Production consists of two laboratories. The Laboratory of Silicon Technology is involved in the manufacture of silicon wafers of the diameters ranging from 1 to 4 inches and the thicknesses from 50 micrometers to over 40 000 micrometers and with different crystallographic orientations, after having them cut, etched and polished (one-side or double-side). In the Laboratory of Epitaxy, silicon epitaxial wafers and multilayer epitaxial structures, such as p/n/n+, n/p/p+, etc. are fabricated using the CVD method. These structures are characterized by the epitaxial layers of a thickness in the range of 2-150 micrometers and resistivity in the range 0.003-1000 Ω cm. The research activity of the Department is also focused on the examination of defects in wide band-gap semiconductors.

The Department of Functional Materials is involved in the fundamental and applied research in the field of crystal growth, new composite materials and the methods of their characterization. The technologies concerning the growth of oxide single crystals, $A^{III}B^{V}$ compounds, as well as 4H- and 6H-SiC are being developed. The scientists in the Department also utilize the micro-pulling-down to examine the growth of metamaterials, plasmonic materials and eutectic systems. The services offered here include the development of crystal growth technologies and the processes of mechanical processing (the manufacture and a proper surface treatment of the obtained materials).

The Laboratory of Structural Research and Materials Characterization carries out fundamental and applied research on the physical properties of materials. These investigations are devoted to the development and improvement of new methods of material analysis and their modification with the use of ion beams. The goal is to improve the structural and functional properties of new materials.

The Laboratory specializes in:

- surface analysis of the materials using scanning electron microscopy (SEM) and other techniques, such as: EDS, EBSD, CL, FIB, which are coupled with a scanning electron microscope,
- structural testing with the use of advanced X-ray diffraction methods (XRD) and high-resolution secondary ion mass spectrometry (SIMS),
- development of the numerical methods for the analysis of data obtained by X-ray diffraction and high-resolution secondary ion mass spectrometry (SIMS),
- development of the methods of material modification using ion beams,
- analysis of the radiation defects in the materials applied in nuclear engineering,
- testing the functional properties of the irradiated polymers,
- examination of the tribological properties (the processes of wear and friction) of various materials.

The Electron-beam and nanoimprint laboratory deals with the manufacture of micro- and nanostructures in the processes of electron-beam lithography (the generation of structure patterns) and nanoimprint (replicas of 3D structures). Thanks to the Micro and Nanotechnology Center MINOS project it has been possible to equip the Laboratory with a Vistec SB251 electron beam lithography system, which is a fully autonomous, professional apparatus, allowing high-resolution patterns (less than 50 nm) to be written over a large area (175 mm × 175 mm) with the address grid of 1 nm. In the laboratory the standard masks are fabricated to be used in other lithographic techniques, i.e. UV lithography (contact photolithography), DUV lithography (optical projection type lithography) and nanoimprint. The electron-beam lithography is also used for a direct generation of the patterns on a variety of semiconducting substrates and optical substrates, which makes it possible to produce electronic and photonic micro- and nanostructures as well as complex diffractive optical elements with the features as small as 50 nm.

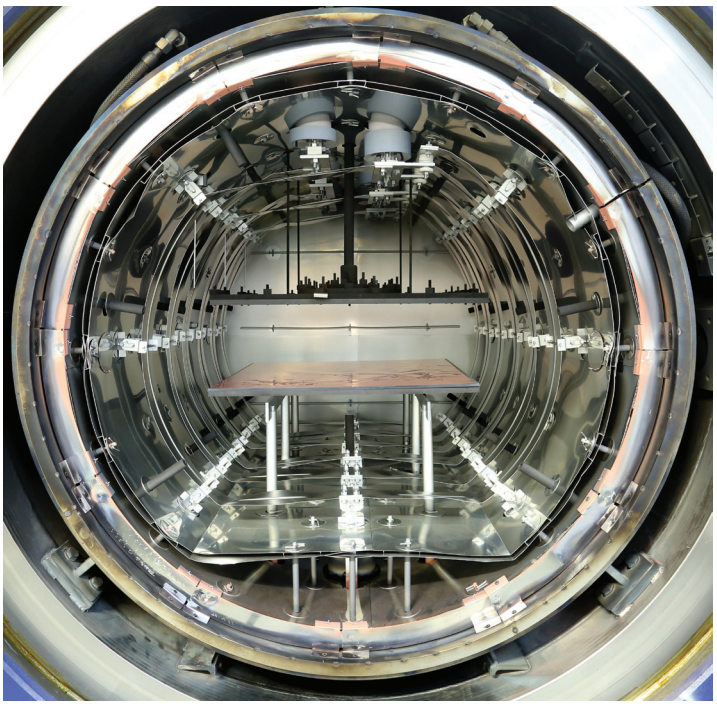

RESEARCH WORKS IN LABORATORIES OF ŁUKASIEWICZ - ITME

The researchers in ŁUKASIEWICZ - ITME are currently involved in tens of scientific projects, i.e. Polish and European projects as well as those carried out under the Horizon 2020 Framework Program for

Research and Innovation. The examples of the undertakings being prepared at the Institute are presented below.

The researchers perform the tasks within the framework of 10-year Graphene Flagship Programme funded by the European Commission. An international scientific-industrial consortium, consisting of nearly 150 partners from 21 countries, carry out a wide range of objectives, from the production of materials and sub-assemblies to the construction of integrated systems. The goal of the project is the development of scientific research devoted to the utilization of graphene and other two-dimensional (2D) materials in various areas of life and economy. Graphene Flagship Programme belongs to one of two projects that won the contest of the Future and Emerging Technologies (FET) Programme. The European Commission has allocated a sum of almost 1 000 000 000 EUR to the implementation of both of these projects.

The team at the Department of Functional Materials is involved in a project carried out by an international consortium (whose member is ŁUKASIEWICZ - ITME), under the name ENSEMBLE3 (Center of ExcelleNce for nanophotonicS, advancEd Materials and novel crystal growth-Based technoLogiEs) within a framework of the program Horizon 2020 - Teaming for Excellence. The purpose of the first phase of this undertaking is the preparation for setting up the Center of Excellence, where new, advanced materials will be developed on the basis of crystal growth technologies, including the materials to be applied in the sectors of nanophotonics, optoelectronics, telecommunications, medicine and photovoltaics. In principle, The Center of Excellence should compete with the leading global scientific institutions, both in terms of innovativeness and mastery in research and development. The ENSEMBLE3 project is carried out by a consortium consisting of: the University of Warsaw, Łukasiewicz Research Network - Institute of Electronic Materials Technology, the National Center for Research and Development, Karlsruhe Institute of Technology (Germany), the nanoGUNE Cooperative Research Center (Spain) and the Sapienza University of Rome (Italy).

The Department of Composite and Ceramic Materials, being a part of an international consortium is involved in a M-ERA.NET program, concerning innovative Ni-Cr-Re coatings with the increased corrosion and erosion resistance for the high-temperature applications in power industry. Within a framework of the project new coatings will be developed based on nickel and chromium metal powders with the additive of rhenium, and an optimal technique for their deposition on steel substrates will be selected.

The Institute also implements an investment program, named “the Centre of Graphene and Innovative Nanotechnology”, related to the purchase of modern research equipment that will allow our scientists to carry out a variety of the innovative scientific projects associated with graphene and other nanomaterials. This undertaking is financed from Structural Funds of the European Union (RPO WM for the years 2014-2020).

SCIENCE IN PRACTICE

Fundamental and applied research is carried out in the laboratories of the Institute. The offer of the Institute includes technologies such as: graphene-based magnetic sensors for industrial applications, power devices based on SiC - i.e. high-voltage diodes, on silicon carbide, high-frequency power devices based on GaN, graphene flakes, crystals, optical waveguides, lasers, white light sources, chromium masks and diffractive elements, multijunction solar cells with enhanced efficiency. We also point out that the development work is in the field of materials engineering and our scientific community is open to solving material problems. The work carried out in the ŁUKASIEWICZ - ITME laboratories results in the technologies that can be commercially applied. Some selected examples are described below:

Graphene magnetic field sensor

At the Department of Graphene and Materials for Electronics, the scientists develop the construction of an innovative magnetic field sensor (named “hallotron”) utilizing the patented technology of graphene deposition on silicon carbide (SiC). The research is carried out in two ways, so that the optimum maximum working temperature and sensitivity can be reached. The first type of a sensor maintains its electrical parameters up to +300°C with a sensitivity of 160 V/AT (volts per ampere-tesla).

The second one exhibits a lower sensitivity (80 V/AT), however, it is maintained at a higher temperature, i.e. even up to +500°C. Such a temperature range is much wider than the temperature characteristic of the conventional devices made of semiconductor materials, such as silicon, gallium arsenide, indium arsenide or indium antimonide. Potentially, this solution could be applied, for instance, in the construction of brushless DC electric motors (BLDC) with the permanent magnets powered by direct voltage or permanent magnet synchronous motors (PMSM) powered by alternating voltage. These types of motors can also be used in electric vehicles, numerically controlled machine tools and in the measuring devices of the new range of current transducers, as well as in single-phase and three-phase active power transducers. An additional advantage of the graphene sensor is the possibility of its operation at low temperatures. The experiments have confirmed that both types of sensors exhibit the sensitivity stability of -0.02%/°C in the temperature range from -200°C to +300°C. This record stability of the electrical parameters within a wide temperature range is the distinctive feature of graphene deposited on silicon carbide. The technology was awarded a silver medal at the 13th International Warsaw Invention

Show IWIS 2019. ŁUKASIEWICZ - ITME is planning to introduce their sensors into a commercial offer.

Production technology of graphene on metallic substrates

Simultaneously with the development of the technology of graphene deposition on silicon carbide, the team at the Department of Graphene and Materials for Electronics aims to establish a method of graphene deposition on a copper foil and on germanium. The graphene produced in such a way can further be transferred onto another material by applying a variety of technological processes. ŁUKASIEWICZ - ITME has gained international recognition due to the very high quality of the graphene transferred, which guarantees purity and predictable electrical parameters of the material. The offer of the Institute includes both small samples and larger graphene sheets. So far, the purchasers have most often ordered a copper foil coated with graphene, with dimensions 30 cm × 30 cm, but the foil measuring 50 cm × 50 cm is also available. As a research institute developing the electronic materials technology on the basis of its own initiatives and projects carried out in the cooperation with foreign and national centers, ŁUKASIEWICZ – ITME work on the implementations that can utilize graphene. So far, projects such as a femtosecond laser or transparent heaters have been successfully completed.

Graphene Ink

The Department of Chemical Synthesis and Graphene Flakes is involved in the manufacture of various nanomaterials and nanostructures, e.g. graphene flakes. The global research in this field has been conducted for only a few years. However, regarding the graphene applications, the Institute has already achieved first implementations.

The development of graphene ink belongs to one of the examples of an effective implementation of the research work carried out in ŁUKASIEWICZ - ITME in cooperation with the Electro-technological Society Qwerty. The obtained graphene ink enables printing on polymer matrices by a jet printing method, including also elastic and translucent materials. The printed layer is homogeneous and highly transparent. After proper treatment, graphene ink becomes electrically conductive. Therefore, the obtained printout can be applied in foil keyboards for the device drivers. Even the use of a small amount of graphene in the ink will enable the replacement of an expensive indium tin oxide (ITO), which is commonly used as a transparent electrical conductor.

Fiber microprobe for selective electroporation of the internal organs and single cells.

The fiber microprobe is a new therapeutic tool, dedicated to electrochemotherapy of internal organs by the laparoscopic techniques. This technology is currently commercialized. The method utilizes the phenomenon of electroporation, i.e. the electrically stimulated formation of short lived nanopores in a cell membrane, which can enable the drug delivery into the cells. Electrochemotherapy is one of the modern methods of cancer treatment.

The fiber microprobe is the only method that enables the electroporation of limited areas in hard-to-reach places. The form of a thin fiber allows the probe to easily reach the inaccessible locations in the body with the help of a needle or through the blood vessels. Simultaneously, the local delivery of drugs is possible, including very toxic or expensive ones. With a built-in imaging channel, this tool also enables a direct observation of the area being electroporated.

The electroporation microprobe was developed by the research team headed by Prof. D. Sc. Ryszard Buczyński. The technology was awarded a silver medal at the 9th International Warsaw Invention Show IWIS 2015. It also received the Polish InnoStars Award in 2016, in MedTech category (medical devices), which is awarded for the innovative projects in the field of health, medicine and biotechnology. The described technology also gained the distinction in the Polish Product of the Future competition (19th edition) in the category: Product of the Future of a scientific unit.

Transparent ceramics

The investigations aimed at obtaining transparent ceramics based on yttrium-aluminum garnet ($Y_3A_{l5}O_{12}$) and magnesium aluminum spinel ($MgAl_2O_4$) are carried out at the Department of Composite and Ceramic Materials. These materials can be used both as transparent armor elements, domes and protective visors for the infrared detectors. Transparent ceramics can also serve as matrices for rare earth elements and transition metals, and hence, after doping, it can be used as a non-linear absorber for the laser beam modulation, an active laser medium in solid-state lasers, and as a converter in white light laser sources.

Luminescent materials for highly efficient white light sources

At the Department of Optoelectronics and Department of Composite and Ceramic Materials, white light sources are developed using ceramic luminescent materials stimulated by blue high-power laser diodes. Our ceramic phosphors are based on yttrium aluminum garnet doped with cerium (YAG: Ce; $Y_3A_{15}O_{12}$: Ce^{3+}) and are obtained in the form of a granulated product in various matrices, layered ceramics and ceramic composites. The controlled change in the microstructure of ceramics, the choice of the appropriate geometry, composition and manufacturing process parameters enable the preparation of the source characterized by the required color and high efficiency. The applications include laser headlights, which are one of the most modern solutions in the automotive industry, energy-efficient street lighting, high-power special-purpose light sources (e.g. medical lamps) and various types of light panels.

CAPACITY IN SCIENCE AND TECHNOLOGY

The Institute has a research potential and the devices. In its possesion are unique on a regional scale. The laboratories at the Centre of Graphene and Innovative Nanotechnology, with the specialized equipment, are the representative examples. High-tech research conducted and the advanced materials and structures are being developed in our numerous departments and laboratories. Our equipment and instruments allow the obtained materials and components to be thoroughly characterized.

The results of the investigations conducted at the Institute are important in both fundamental and applied aspects. For decades, our scientists have published the research articles in leading international scientific journals. For instance, in the years 2013-2017 over 460 reports, whose co-authors are ITME employees, were published in the peer reviewed journals belonging to Master Journal List. Our researchers are also the inventors of tens of patents and numerous patent applications.

Over the years, the achievements of ŁUKASIEWICZ - ITME have been appreciated. The Institute has appeared in the ranking of the most important scientific institutions in the world, i.e. SCImago Institutions Rankings. In 2019, it was placed on 7th position among the best state-owned scientific units in Poland and on 20th position in Eastern Europe.

Thermal conductivity /diffusivity measurements

The Department of Composites and Ceramic Materials

LFA 457 Micro Flash NETZSCH

Facilities:

- LFA 457 Micro Flash NETZSCH equipment is applied for thermal diffusivity measurements. The front side of a plane parallel solid sample is heated by a short laser pulse.
- The temperature rise on the rear surface is measured versus time using an infrared detector.
- Compared with the direct measurements of thermal conductivity, this method has an advantage of a simple test piece configuration, small test piece size, applicability to a wide range of diffusivity values, great accuracy and reproducibility.

Parameters:

- Temperature range: RT - 1100°C
- Thermal Diffusivity range: 0.01 mm^2/s to 1000 mm^2/s
- Thermal Conductivity range: 0.1 W/(m·K) to 2000W/(m·K)

Sample size:

- Rectangular (8.0x8.0 mm or 10.0x10.0 mm)
- Cylindrical (10.0 mm, 12.7 mm, 25.4 mm)

RESEARCH NETWORK ŁUKASIEWICZ

Insitute of Electronic Materials Technology

Wólczyńska 133,
01-919 Warszawa

+48 22 835 30 41
+48 22 639 58 05

itme@itme.edu.pl
komercjalizacja@itme.edu.pl

INFORMATION FOR AUTHORS AND READERS

I. Submission rules

1. Only the manuscripts not published previously can be accepted. The author of the paper or the person submitting the manuscript of a multi-author work on behalf of all co-authors are required to declare that the work has not been published previously. If the test results contained in the manuscript have been presented earlier at a scientific conference or a symposium, the information on this fact should be given at the end of article containing the name, place and date of the conference. At the end of the article the authors should also provide the information on the sources of a financial support of the work, the contribution of scientific and research institutions, associations and other entities.

2. The manuscripts both in Polish and in English can be submitted. Due to introducing all the articles printed in *Electronic Materials* to the Internet , the author should make a statement on the copyright transfer of the author's economic rights to the Publisher.

3. Concerned about the reliability of the scientific work and the development of an ethical attitude of a researcher, a procedure has been introduced in order to prevent any cases of scientific dishonesty and unethical attitudes, defined as *ghostwriting* and *guest authorship* (*honorary authorship*):

- *ghostwriting* occurs when someone has made a substantial contribution to the publication without revealing his participation as one of the authors or without mentioning his role in the acknowledgments in the publication;
- *guest authorship* occurs when although the contribution of a given person is negligible or it has not taken place at all, he or she is an author/co-author of the publication.

The Editors require that the authors disclose the contributions of the individual authors in the preparation of a multi-author work, giving their affiliations and the information on their participation in the creative process, i.e. the information on the authors of the work's idea, assumptions, methods, etc. that have been utilized during the article preparation. The main responsibility for this information is borne by the author submitting the manuscript.

4. The Editors are obliged to keep the documentation of any forms of the scientific dishonesty, especially the violation of the ethical rules that are obligatory in science. All discovered cases of *ghostwriting* and "guest authorship" will be disclosed by the Editors, including the notification of the relevant entities, such as the institutions employing the authors, scientific societies, associations of scientific editors, etc.

II. Procedure of articles review and approval for print

1. The author's materials directed for print in "Electronic Materials" are subjected to evaluation by the independent reviewers and the members of the Editorial Board.

2. The reviewers are suggested by the thematic editors – the members of the Editorial Board, responsible for a given subject field.

3. At least two independent reviewers from outside the research institution affiliated by the author of the publication are called for the evaluation of each publication.

4. In case of a publication in a foreign language, at least one reviewer is called, affiliated in a foreign institution with the seat in a country other than that of the origin of the author of the manuscript.

5. The author or authors of the manuscript and the reviewers do not know their identities (the so-called "double-blind review process").

6. A review is in written form and contains a clear conclusion of the reviewer concerning the article acceptance for the publication (without corrections or with necessary amendments to be made by the author) or its rejection.

7. The criteria for the article acceptance or rejection and a possible review form are disclosed to the public on the website of *Electronic Materials.*

8. The names of the reviewers of the individual publications or the editions are not disclosed. Once a year, in the last issue of "Electronic Materials", a list of the cooperating reviewers will be made public.

9. The Editors of *Electronic Materials* may edit the material obtained, shorten or supplement it (after an agreement with the author), or not qualify it for the publication.

10. The Editor-in-chief refuses to publish the authors' materials in the following cases:

- the contents of the manuscript are illicit,
- any signs of the scientific dishonesty, and especially *ghostwriting* and *guest authorship*, will be found out,
- the work has not received a positive final evaluation from the reviewers and the thematic editor.

11. The Editor-in-chief may refuse to publish the article if:

- the topic of the work is not in line with the subject field of *Electronic Materials*,
- the manuscript exceeds the acceptable volume and the author does not agree to shorten the article,
- the author refuses to make any necessary amendments proposed by the reviewer and the Editorial Board,
- the text or the illustrations provided by the author do not meet the technical requirements.

LIST OF REVIEWERS 2019

dr hab. inż. Zbigniew Pędzich

dr Anna Wajler

dr Andrzej Swinarew

dr inż. Bartłomiej Wysocki

Abstracs of selected publications of ŁUKASIEWICZ - ITME employees

Three dimensional localization of unintentional oxygen impurities in gallium nitride

P. Michalowski[1], S. Zlotnik[1], M. Rudzinski[1]

[1] Lukasiewicz Res Network, Inst Elect Mat Technol, Wolczynska 133, PL-01919 Warsaw, Poland.

Chemical Communications, 2019, 55, 77, 11539-11542.

Further development of gallium nitride (GaN) based optoelectronic devices requires in-depth understanding of the defects present in GaN grown on a sapphire substrate. In this work, we present three dimensional secondary ion mass spectrometry (SIMS) detection of oxygen. Distribution of these impurities is not homogeneous and the vast majority of oxygen atoms are agglomerated along pillar-shaped structures. Defect-selective etching and scanning electron microscopy imaging complement SIMS results and reveal that oxygen is predominantly present along the cores of screw and mixed dislocations, which proves their high tendency to be decorated by oxygen. A negligible amount of oxygen can be found within the bulk of the material and along the edge dislocations.

Experimental analysis of axial stress distribution in nanostructured core fused silica fibers

A. Anuszkiewicz[1], M. Bidus[2], A. Filipkowski[1], D. Pysz[1], M. Dlubek[2], R. Buczynski[1,3]

[1] Lukasiewicz Res Network, Inst Elect Mat Technol, Dept Glass, Wolczynska 133, PL-01919 Warsaw, Poland
[2] FIBRAIN Sp Zoo, Zaczernie 190F, PL-36062 Zaczernie, Poland
[3] Univ Warsaw, Fac Phys, Pasteura 5, PL-02093 Warsaw, Poland

Optical Materials Express, 2019, 9, 11, 4370-4378.

We experimentally studied axial stress distribution in recently developed optical all-solid fibers with nanostructured cores. In this type of fiber, the core is composed of thousands of low and high refractive index glass rods with individual diameters of a few hundred nanometers. A distribution of nanorods determines the effective distribution of the refractive index in the core. A structure of nanorods may introduce unrevealed axial stress distribution after fiber drawing, which may induce change of the expected refractive index value. We studied stress in a custom made nanostructured silica fiber with parabolic refractive index distribution in the core and compared it with the reference SMF-28 fiber. For nanostructured fibers we proved that the axial stress is purely thermal with negligible contribution of mechanical stress. This results in the presence of tensile stress in the fiber core, which is in contrary to a standard telecom fiber, where a compressive stress in the core exists. We showed that measured axial stress has negligible impact on refractive index distribution of nanostructured fibers, thus it does not affect its performance. (C) 2019 Optical Society of America under the terms of the OSA Open Access Publishing Agreement

Hybrid electrode composed of multiwall carbon nanotubes decorated with magnetite nanoparticles for aqueous supercapacitors

M. Krajewski[1], PY Liao[2], M. Michalska[3], M. Tokarczyk[4], JY Lin[2]

[1] Polish Acad Sci, Inst Fundamental Technol Res, Pawinskiego 5B, PL-02106 Warsaw, Poland
[2] Tatung Univ, Dept Chem Engn & Biotechnol, 40, Sec 3, Chungshan North Rd, Taipei 104, Taiwan
[3] Lukasiewicz Res Network Inst Elect Mat Technol, Wolczynska 133, PL-01919 Warsaw, Poland
[4] Univ Warsaw, Fac Phys, Inst Expt Phys, Pasteura 5, PL-502093 Warsaw, Poland

Journal of Energy Storage, 2019, 26.

This work describes a use of a composite nanomaterial which consists of multiwall carbon nanotubes covered by iron oxide nanoparticles as a hybrid electrode in aqueous supercapacitor. The investigated nanomaterial was manufactured in a two-step simple chemical synthesis in which the first step was a functionalization of carbon nanotubes whereas the second one was the deposition of iron oxide. According the morphological and structural characterization, the carbon nanotubes with diameters of 10-40 nm were successfully covered by randomly-dispersed magnetite nanoparticles with average diameter of 10 nm. Moreover, the thermogravimetric analysis results indicated that the mass ratio between carbon nanotubes and iron oxide nanoparticles was about 65-35%. The electrochemical performance of studied hybrid electrode was tested in 1 M aqueous KCl electrolyte. The highest specific capacitance of 143 F g(-1) was recorded at a discharge current density of 1 A g(-1). The investigated nanomaterial also exhibited excellent cycling stability i.e. 81% retention of the initial capacitance after 3000 cycles.